SUPPORTING INFORMATION

Water soluble Organometallic Small Molecules as Promising Antibacterial Agents: Synthesis, Physical-chemistry properties and Biological Evaluation to tackling bacterial infections.

Ines Bennour,[1] M. Núria Ramos,[2] Miquel Nuez,[1] Jewel Ann Maria Xavier,[1] Ana B. Buades,[1] Reijo Sillanpää,[3] Francesc Teixidor,[1] Duane Choquesillo-Lazarte,[4] Isabel Romero,[5] Margarita Martinez-Medina,[4] Clara Viñas*,[1].

Institut de Ciència de Materials de Barcelona, Consejo Superior de Investigaciones Científicas, Campus Universitat Autònoma de Barcelona, 08193 Bellaterra, Spain Fax: (internat.) + 34-935805729

MicrobiologyMicrobiology of the Intestinal Disease group, Biology Department of Biology, Universitat de Girona, 17003 Girona, Spain.

Departament de Química and Serveis Tècnics de Recerca, Universitat de Girona, C/ M. Aurèlia Campmany, 69, E-17003 Girona, Spain

Dept. of Chemistry, University of Jyväskylä. FIN-40014, Jyvaskyla, Finland.

Laboratorio de Estudios Cristalográficos, IACT, CSIC-Universidad de Granada, Armilla, 18100 Granada, Spain

Table of content

Scheme S1. a) Synthesis in solution of anionic *ortho*-metallabis(dicarbollides) by complexation reaction of the *ortho nido*-carboranyl ligands and the corresponding MCl_2 salt (M= Co and Fe). b) Synthesis in solution of anionic *meta*-metallabis(dicarbollides) by complexation reaction of the *meta nido*-carboranyl ligands and the corresponding MCl_2 salt (M= Co and Fe).[1] Anionic ligands are obtained by "partial deboronation" reaction of the corresponding icosahedral neutral *closo*-carboranes with a nucleophile (Nu^- = EtO^-, pyperidine, F^-, among others).[2] Circles in grey represent the C_c-H vertices, the orange ones correspond to metal (M= Co^{3+}, Fe^{3+}) while the circles in pink correspond to B-H vertices.

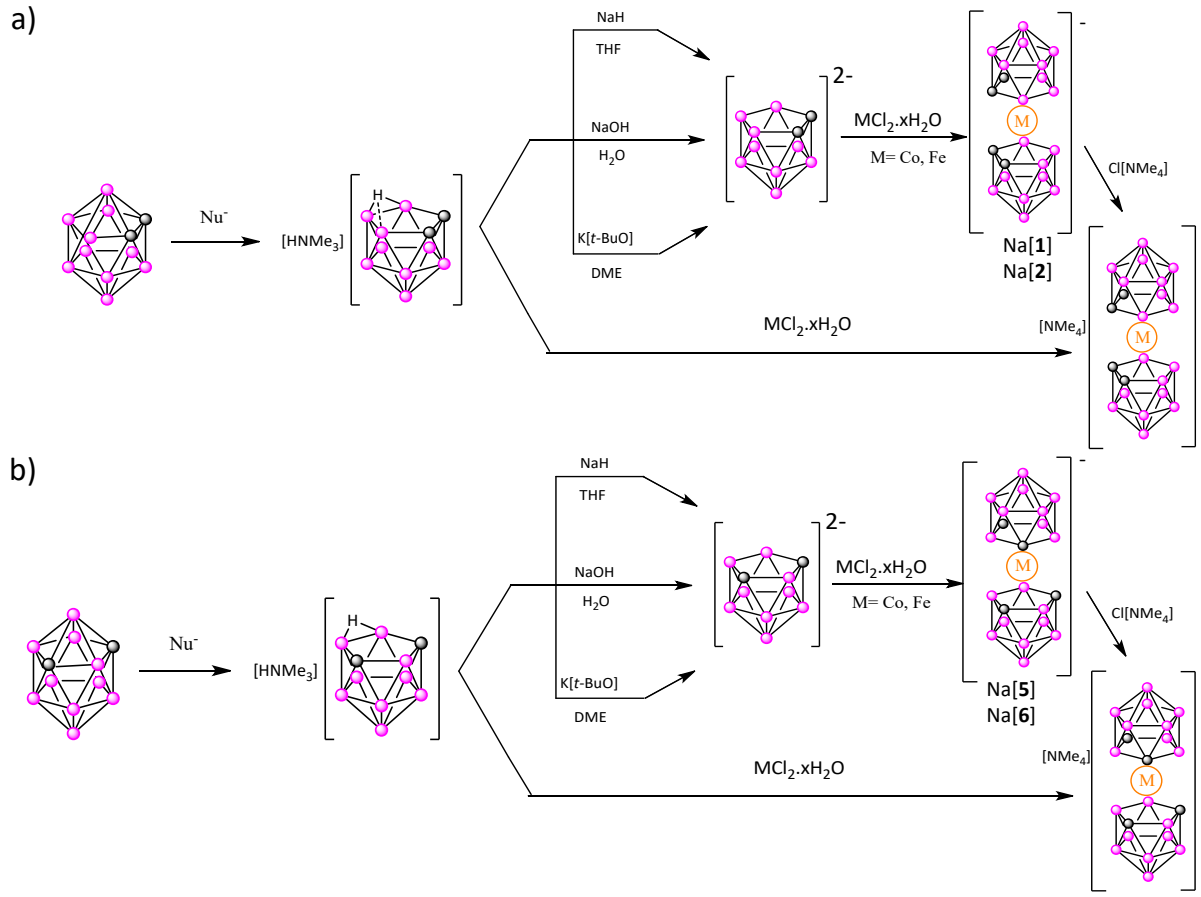

Scheme S2. Synthesis in solid state of $[HNMe_3]^+$ salt of the anionic small cobaltabis(dicarbollide) molecules: a) [**1**]$^-$ and b) [**5**]$^-$ by complexation reaction of the $[HNMe_3]^+$ salt of the corresponding *ortho* and *meta nido*-carboranyl ligands with $CoCl_2.xH_2O$.[3]

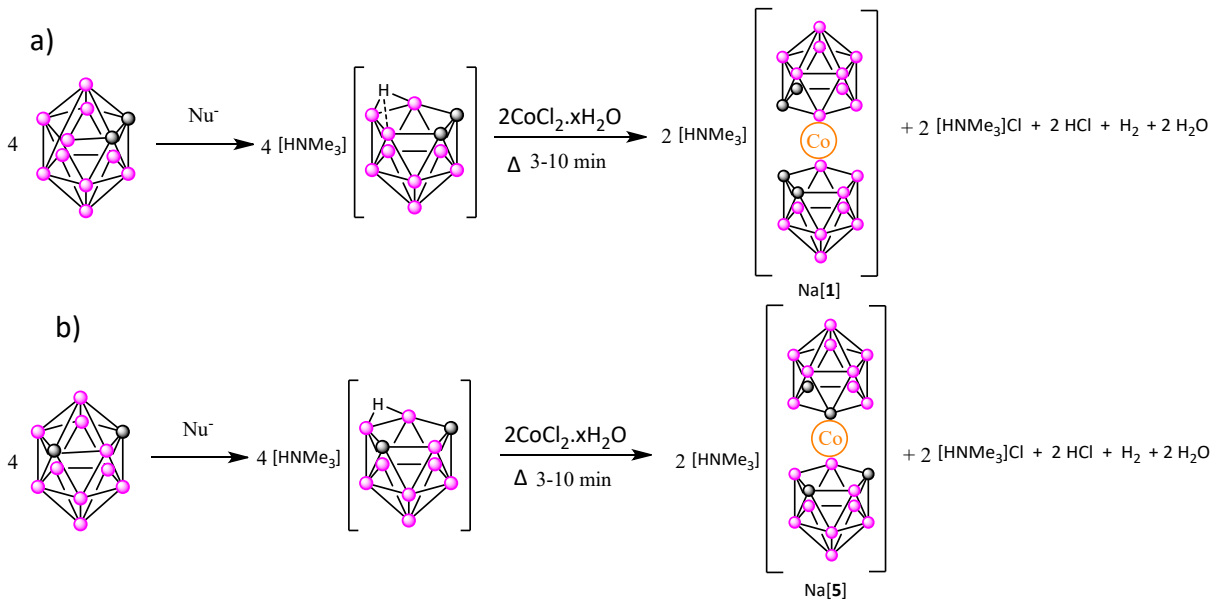

Scheme S3. a) Preparation of the corresponding sodium salts, Na[**1**],[4] and Na[**2**],[5] by cation exchange resin. b) Preparation of the water soluble sodium salts of [**4**]$^-$ and [**5**]$^-$ by means of cationic exchange resin.[6]

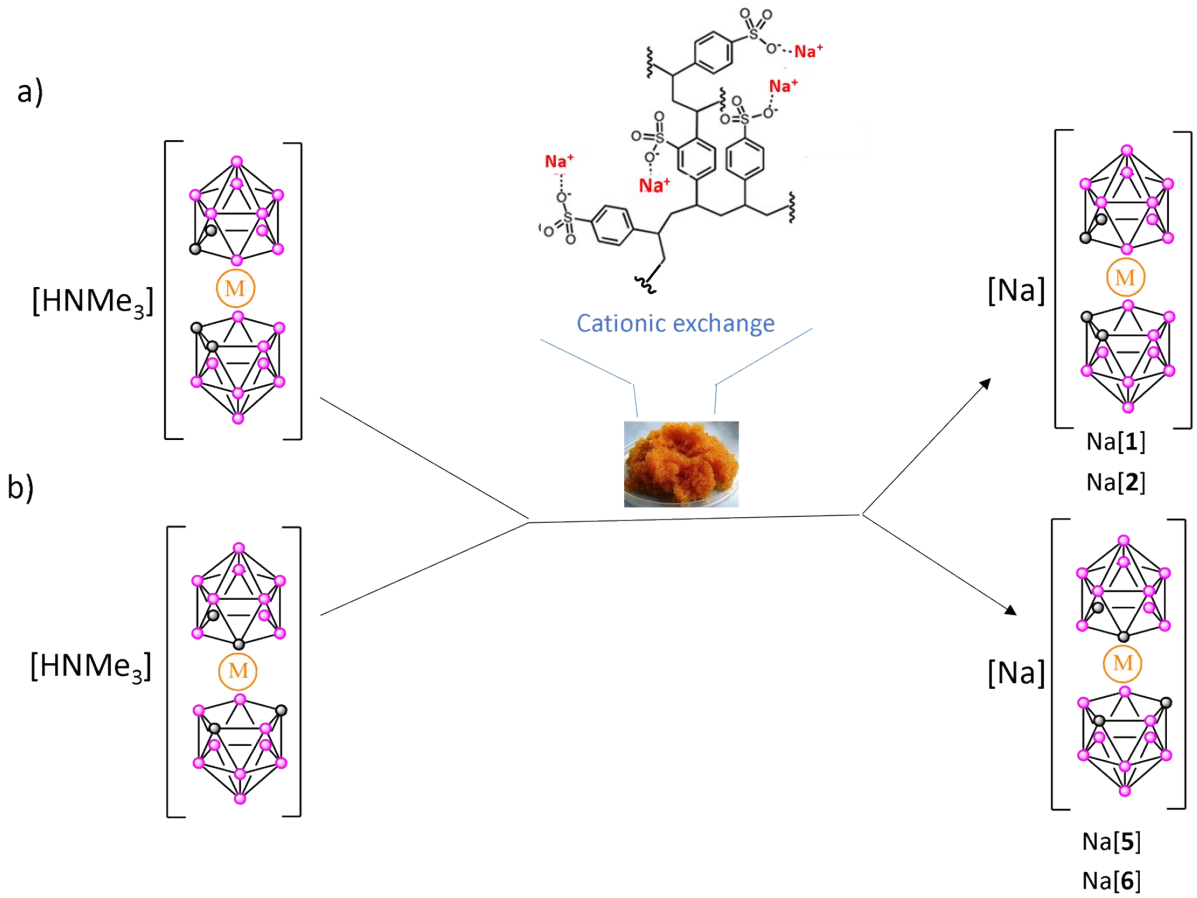

Scheme S4. a) Synthesis of the Cs[**3**] from [**1**]$^-$ employing either ICl (yield = 84%,),[7] or I_2 (yield= 98%)[8] in EtOH at reflux. b) Synthesis of the water soluble Na[8,8′-I_2-*o*-COSAN] by means of cationic exchange resin.

a)

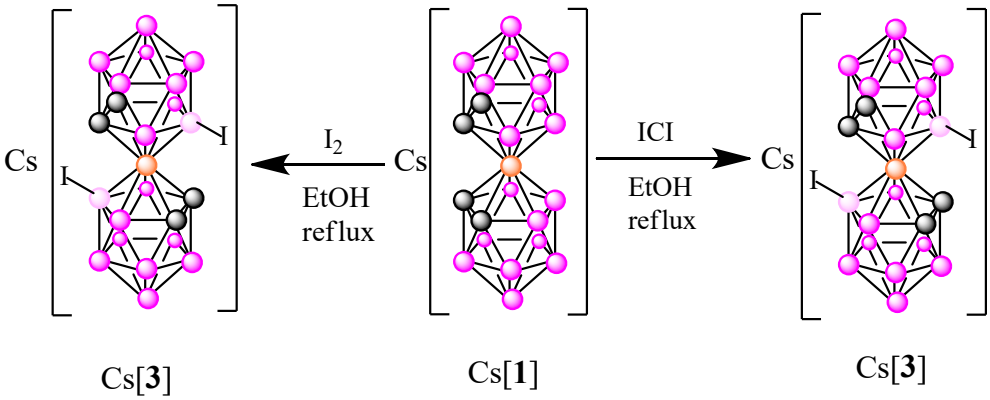

b)

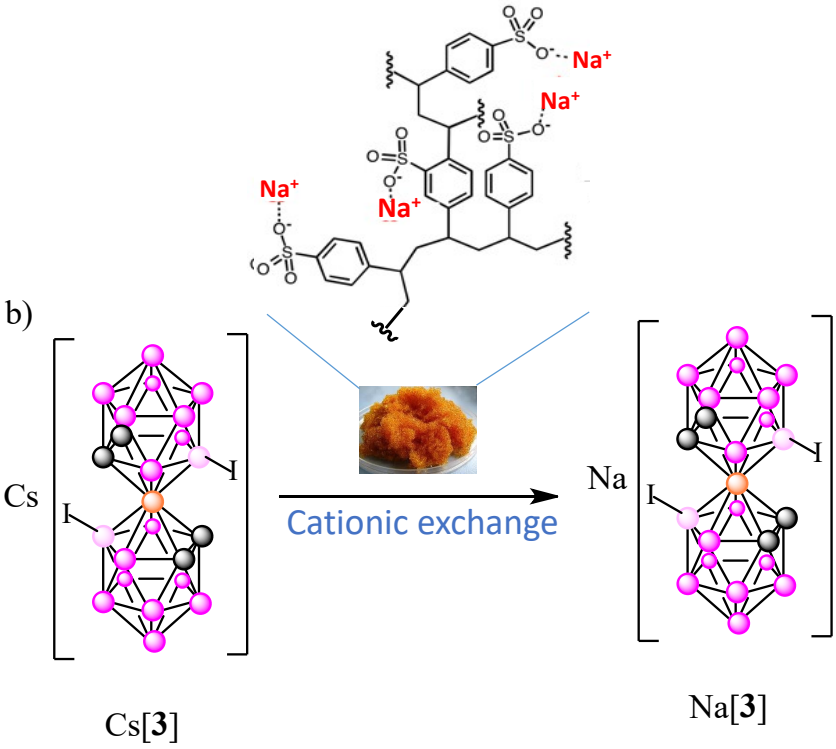

Characterization of Na[2,2'-Co(1,7-$C_2B_9H_{11}$)$_2$]·2.5H_2O, abbreviated as Na[5].

Figure S1. IR spectrum of Na[2,2'-Co(1,7-$C_2B_9H_{11}$)$_2$]·2.5H_2O, Na[**5**].

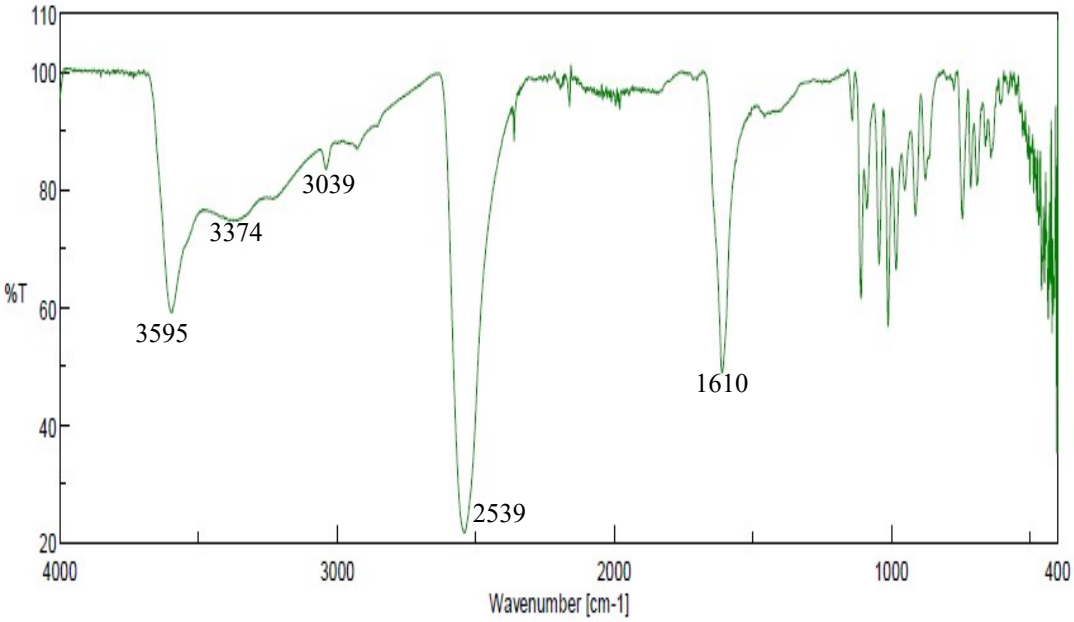

Figure S2. MALDI-TOF-MS experimental spectrum of [**5**]$^-$. Inset the theoretical MS.

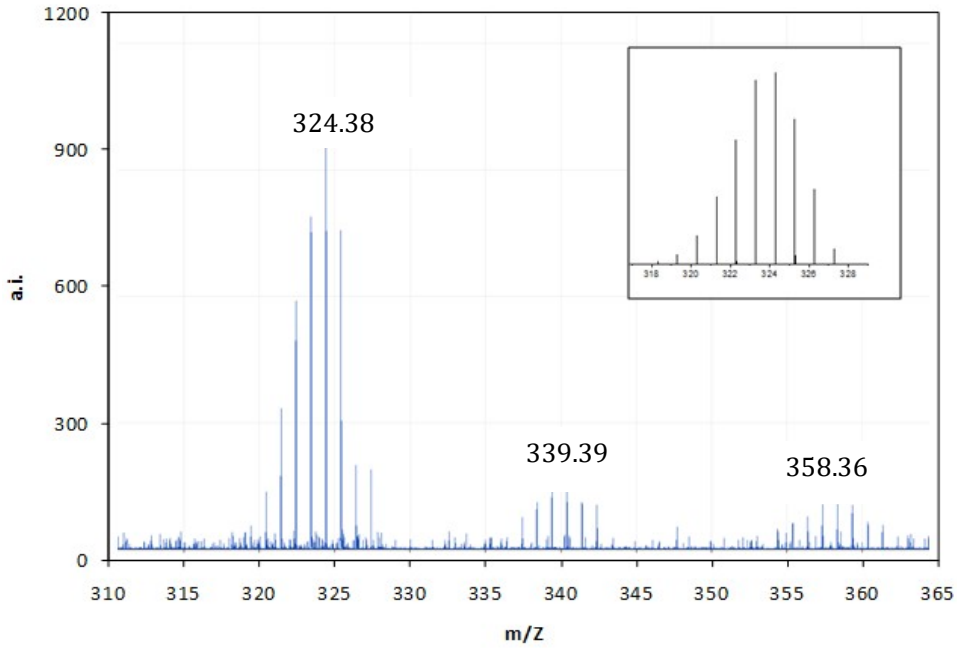

Figure S3. $^{1}H\{^{11}B\}$-NMR of Na[**5**] in D_2O

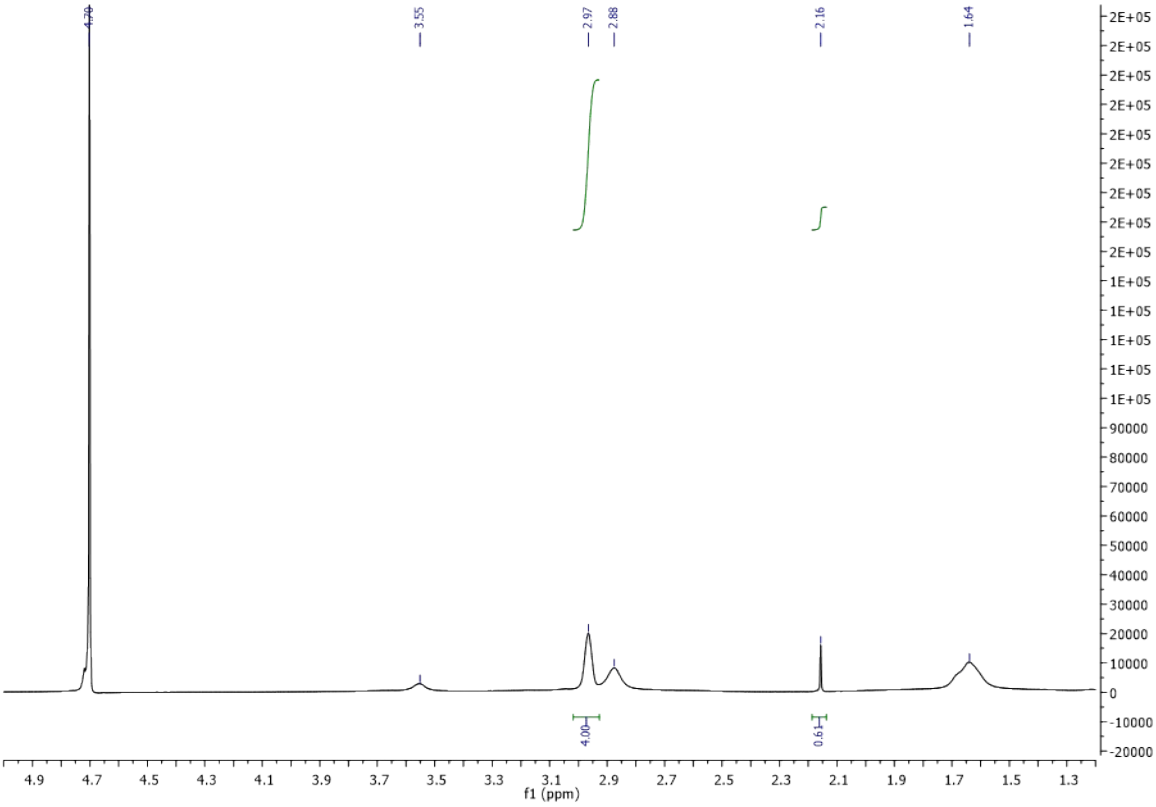

Figure S4. ^{1}H NMR of Na[**5**] in D_2O

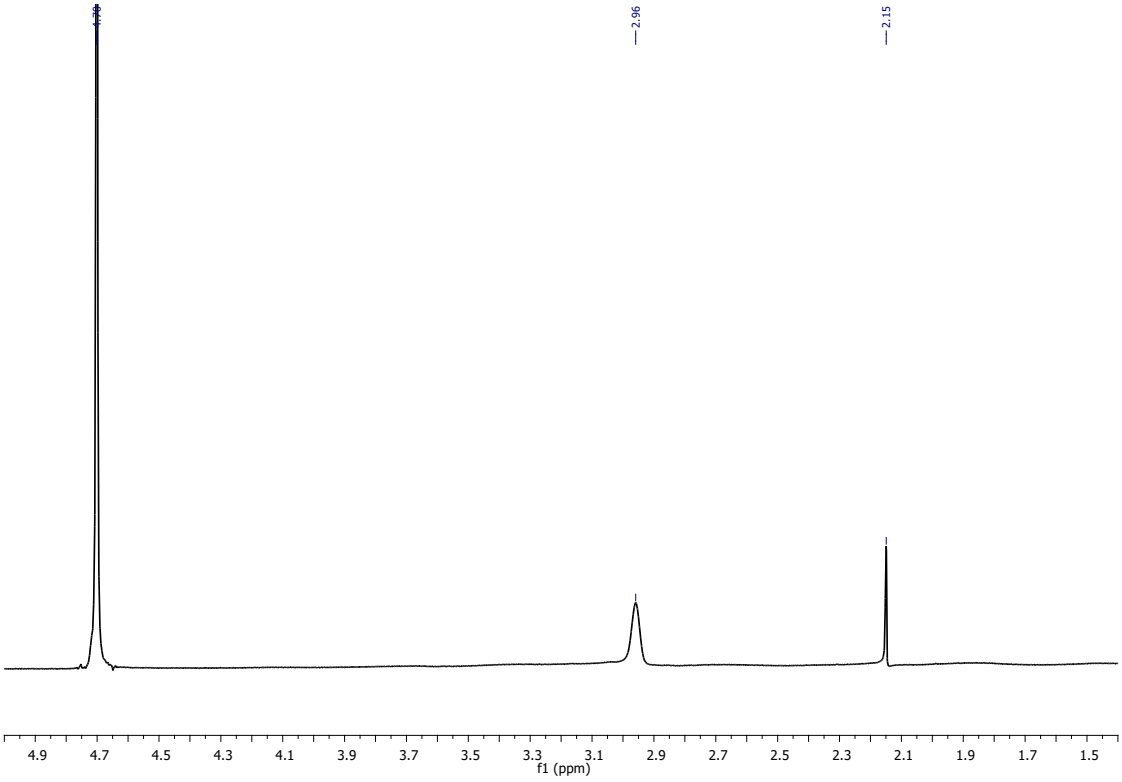

Figure S5. $^{1}H\{^{11}B\}$ NMR of Na[**5**] in CD_3COCD_3.

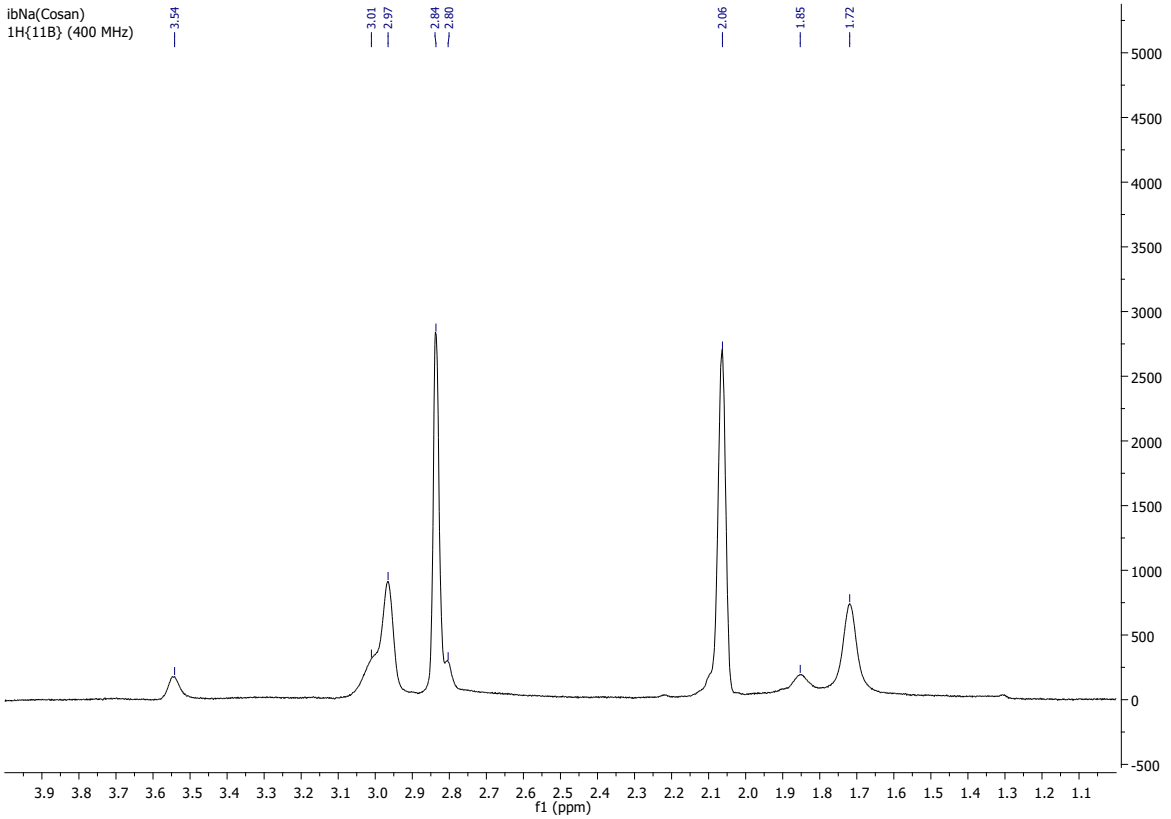

Figure S6. ^{1}H NMR of Na[**5**] in CD_3COCD_3.

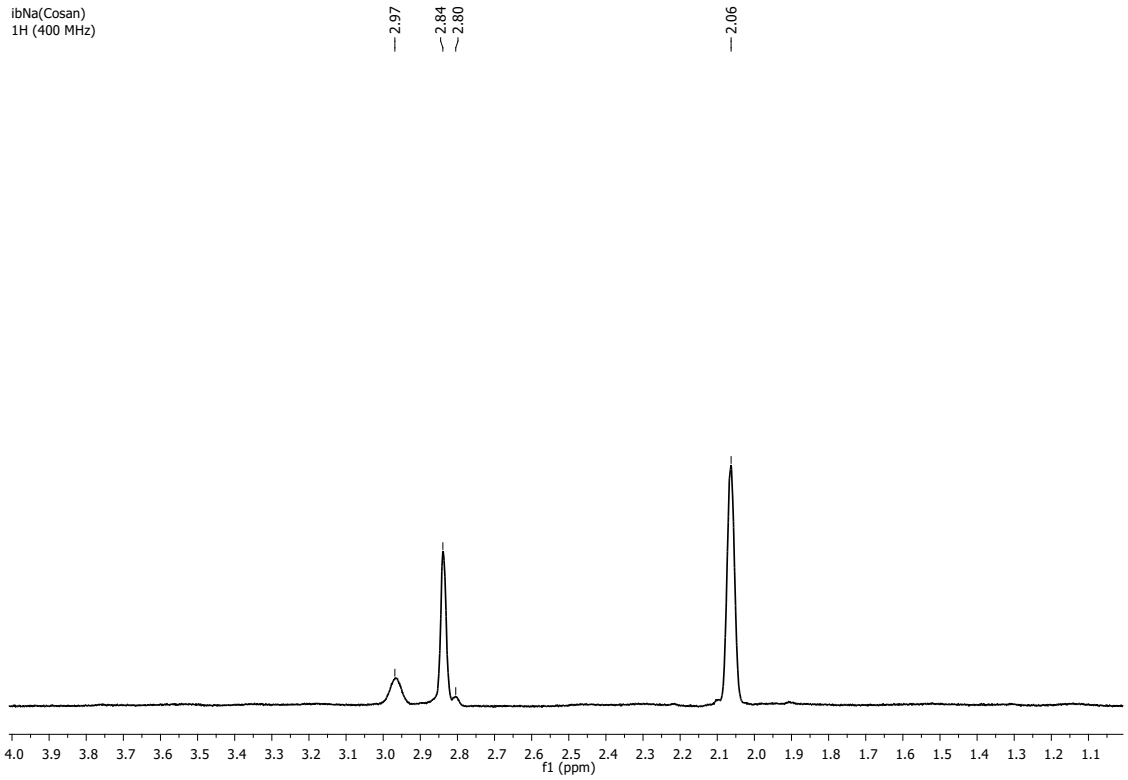

Figure S7. $^{11}B\{^{1}H\}$ NMR of Na[**5**] in D_2O.

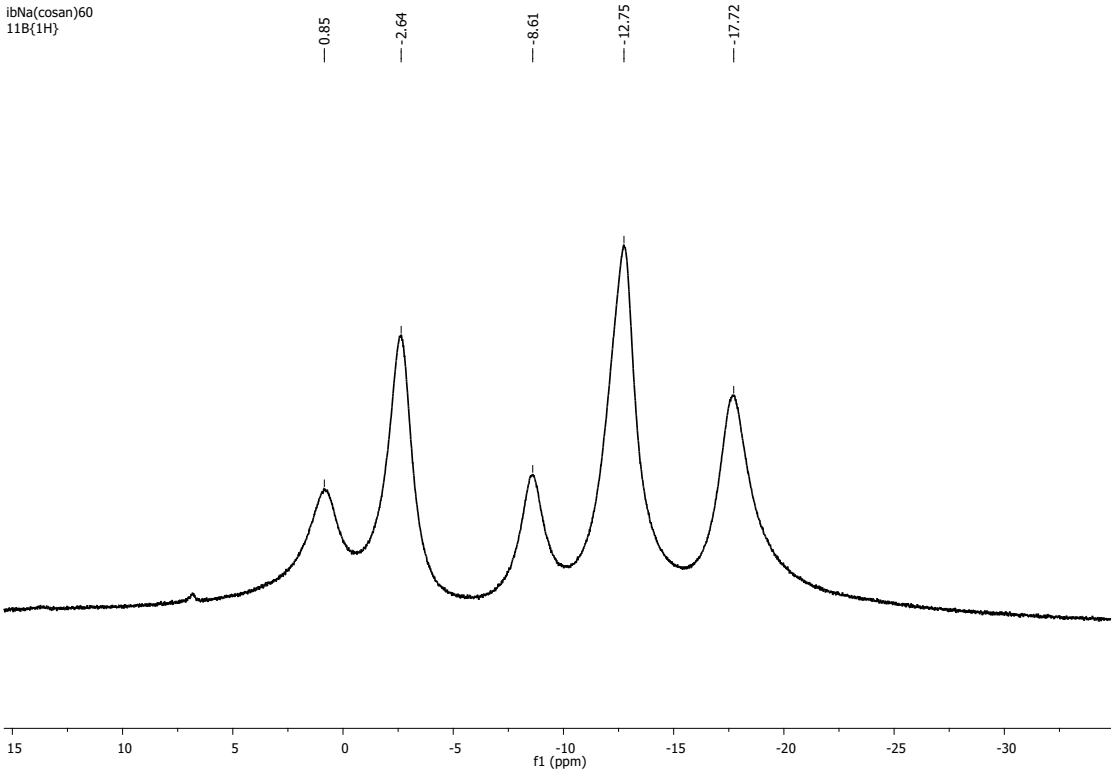

Figure S8. $^{11}B\{^{1}H\}$ NMR of Na[**5**] in CD_3COCD_3.

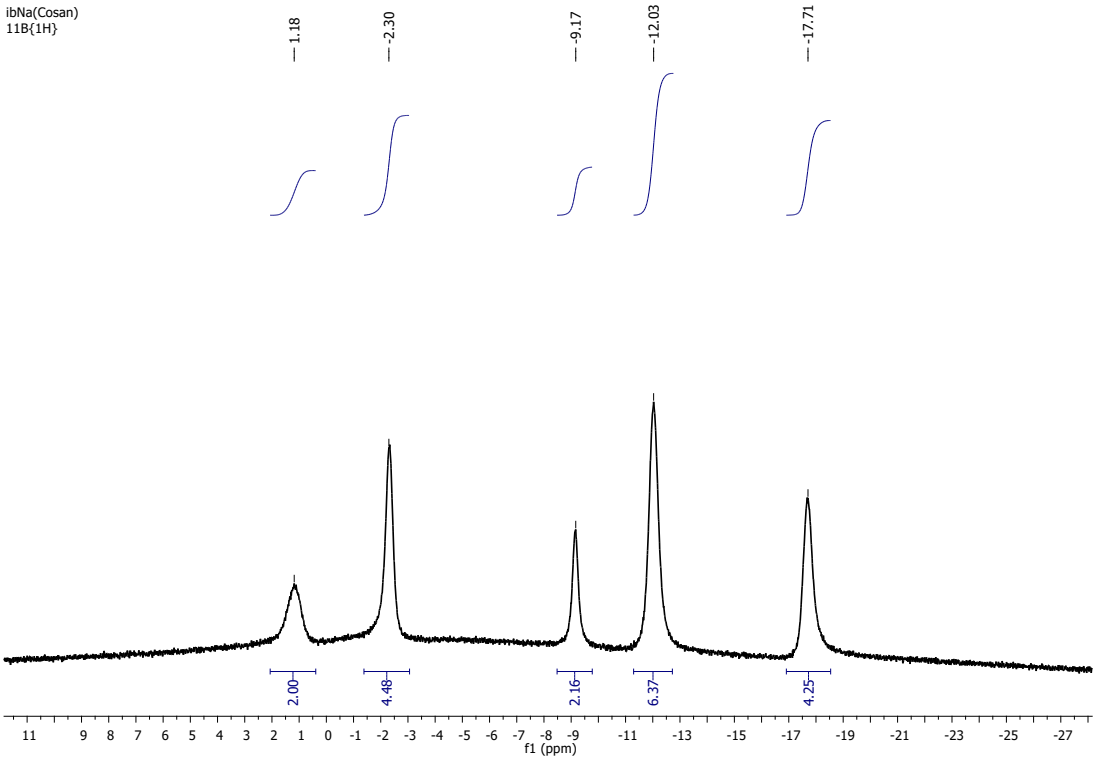

Figure S9. ^{11}B NMR of Na[**5**] in CD_3COCD_3.

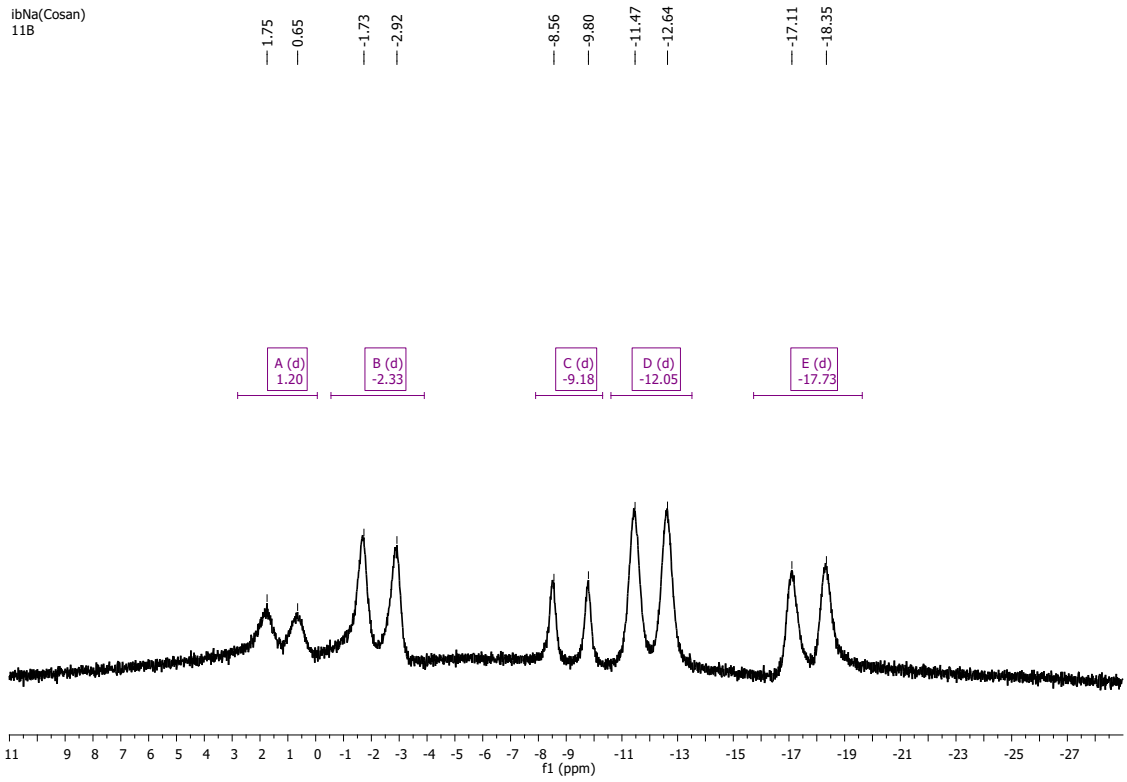

Figure S10. TGA/DSC spectra of Na[**5**].

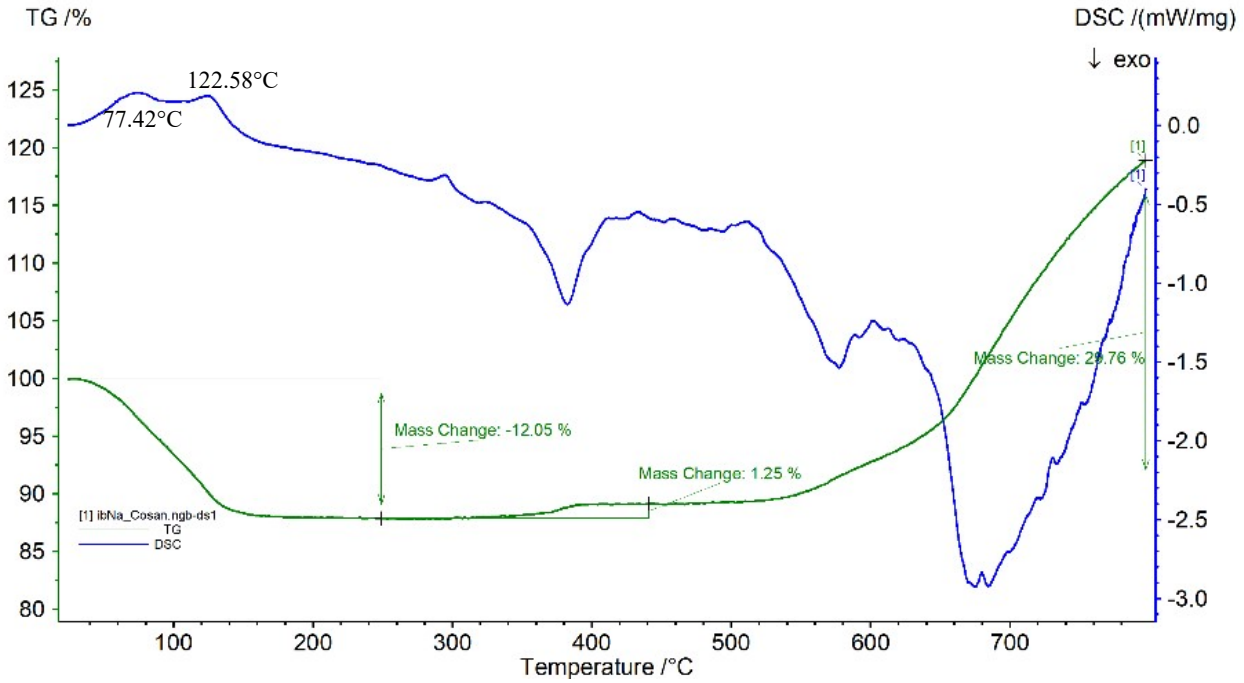

Characterization of Na[2,2'-Fe(1,7-$C_2B_9H_{11}$)$_2$]·2.5H_2O, abbreviated as Na[6].

Figure S11. IR spectrum of Na[2,2'-Fe(1,7-$C_2B_9H_{11}$)$_2$]·2.5H_2O, Na[**6**].

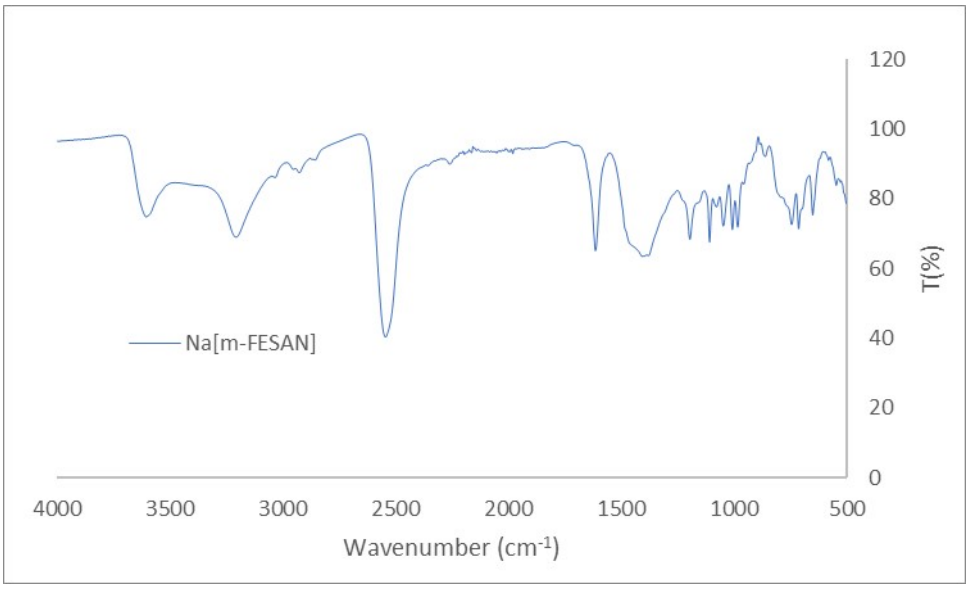

Figure S12. MALDI-TOF-MS experimental spectrum of [**6**]$^-$. Inset the theoretical MS.

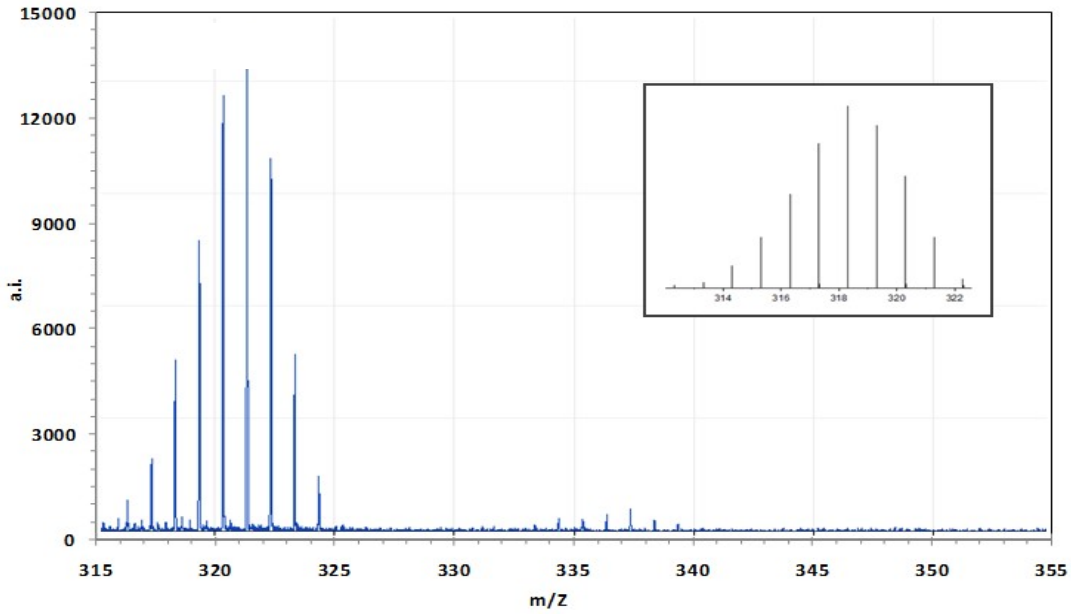

Figure S13. ^{1}H NMR of Na[**6**] in CD_3COCD_3.

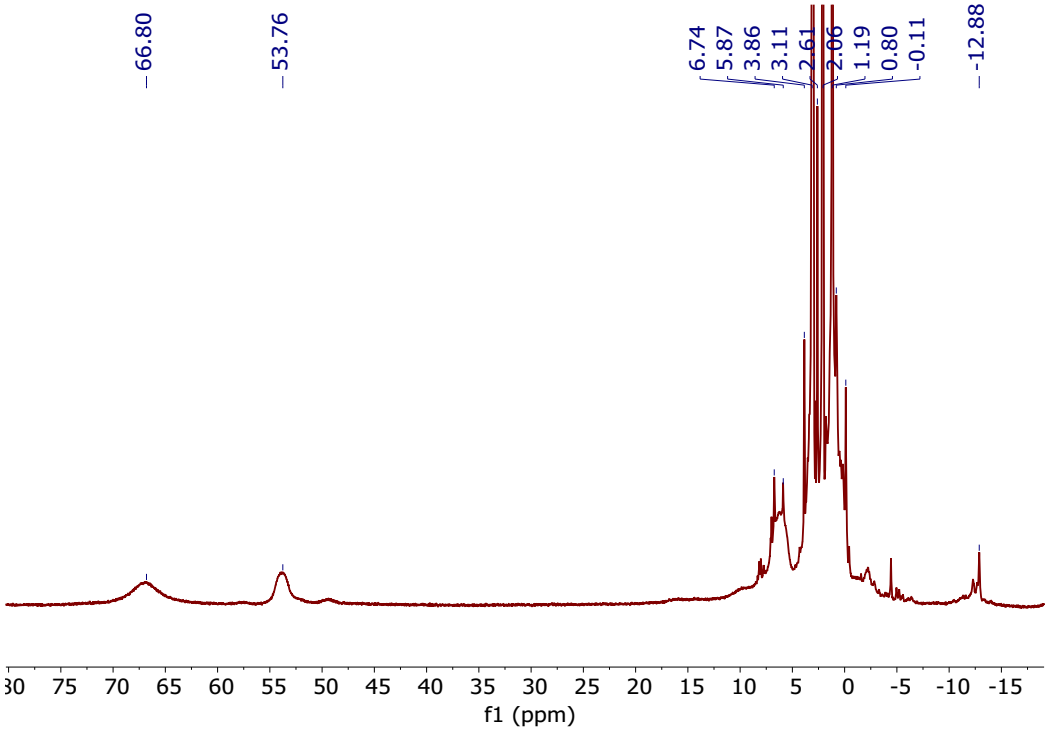

Figure S14. $^{11}B\{^{1}H\}$ NMR of Na[**6**] in CD_3COCD_3.

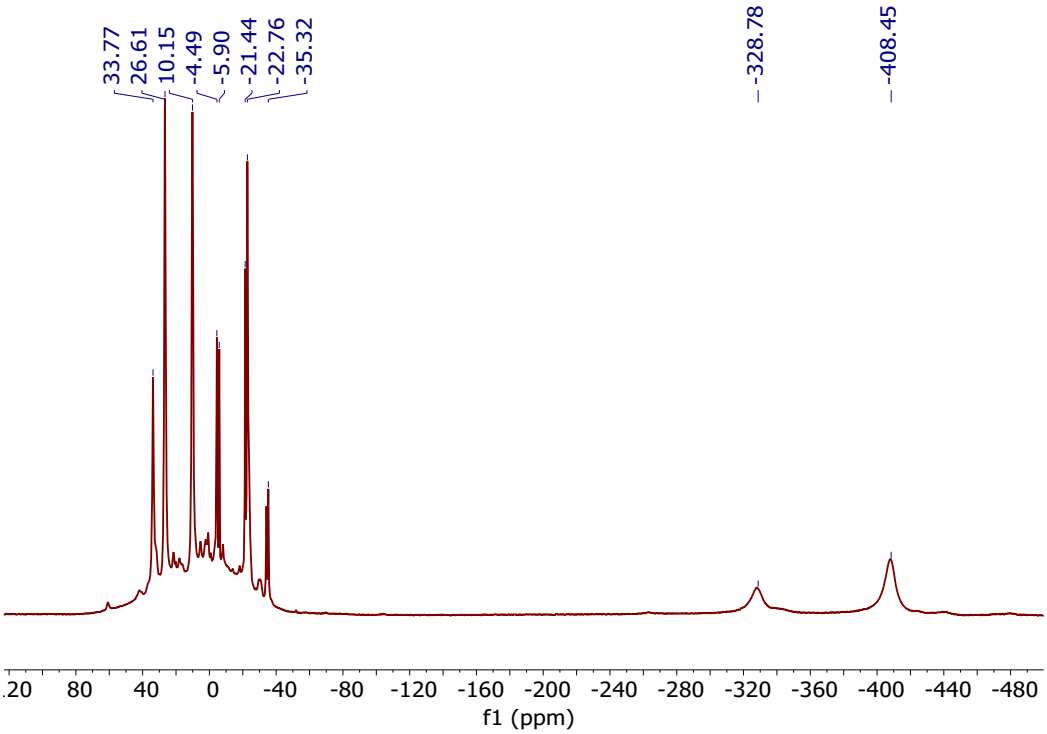

Figure S15. ^{1}H NMR of Na[**6**] in H_2O.

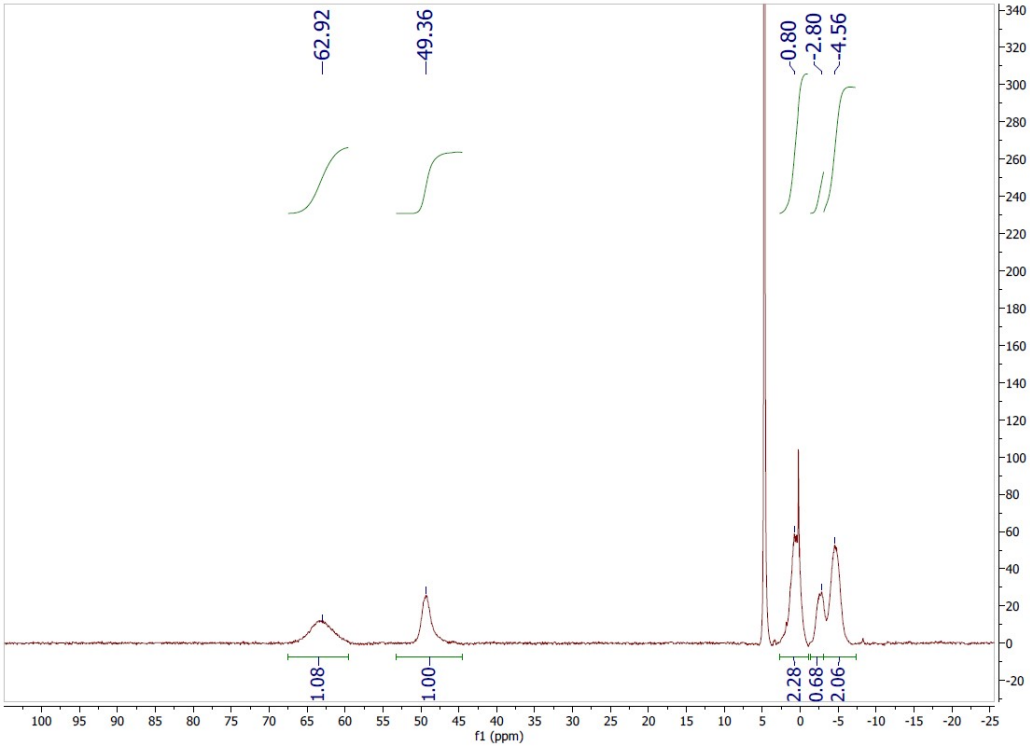

Figure S16. $^{1}H\{^{11}B\}$ NMR of Na[**6**] in H_2O.

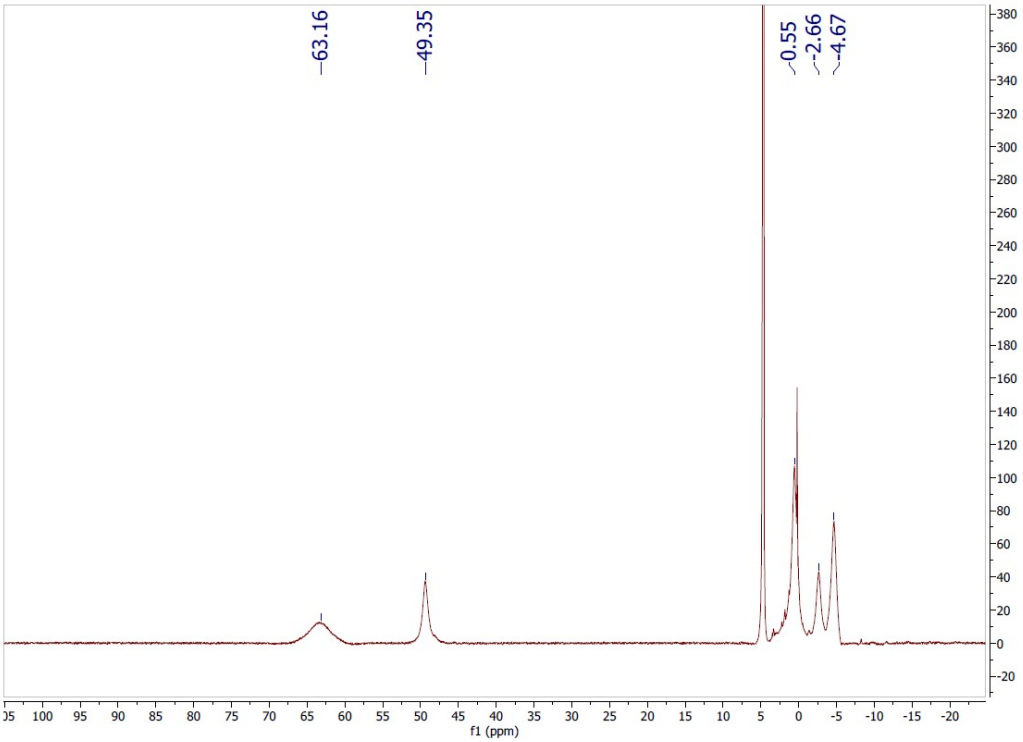

Figure S17. ^{11}B NMR of Na[**6**] in H_2O.

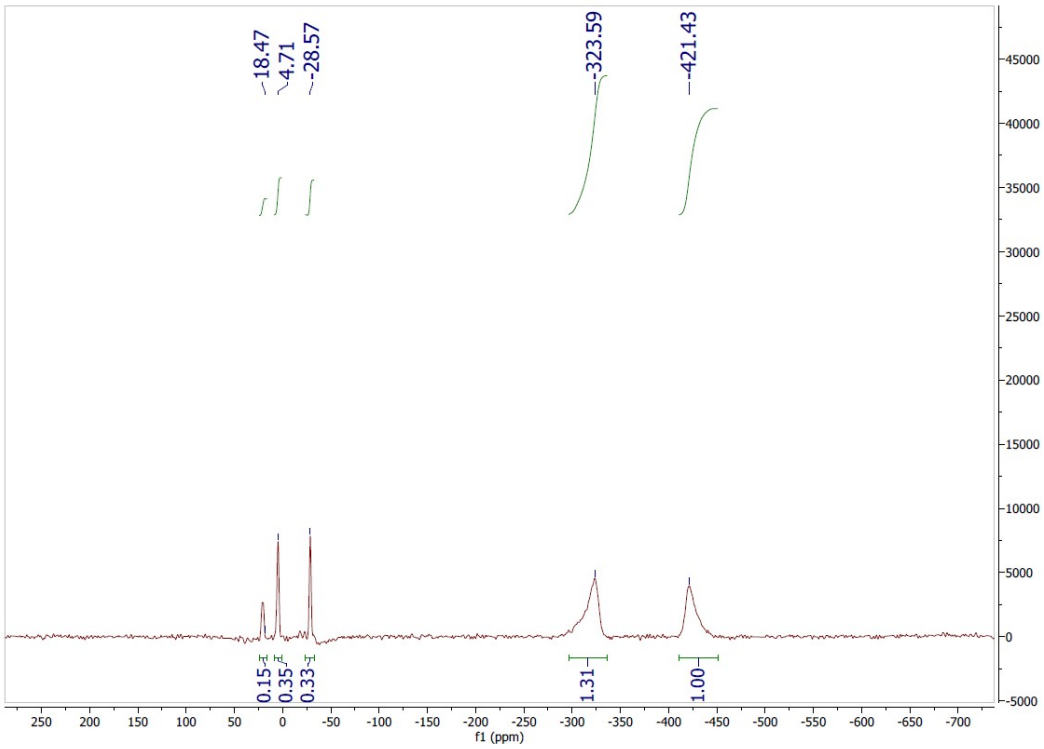

Figure S18. $^{11}B\{^1H\}$ NMR of Na[**6**] in H_2O.

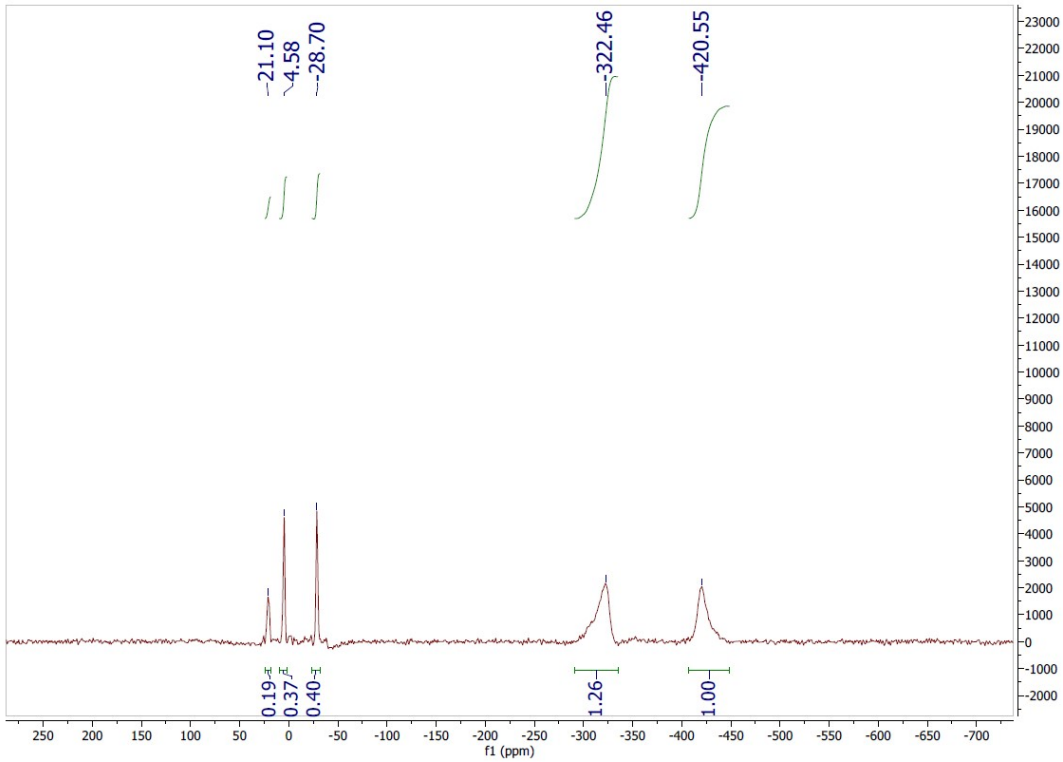

Characterization of Cs[3,3'-Fe(8-I-1,2-$C_2B_9H_{11}$)$_2$, abbreviated as Cs[4].

Figure S19. MALDI-TOF-MS experimental spectrum of Cs[**4**]. Inset the theoretical MS.

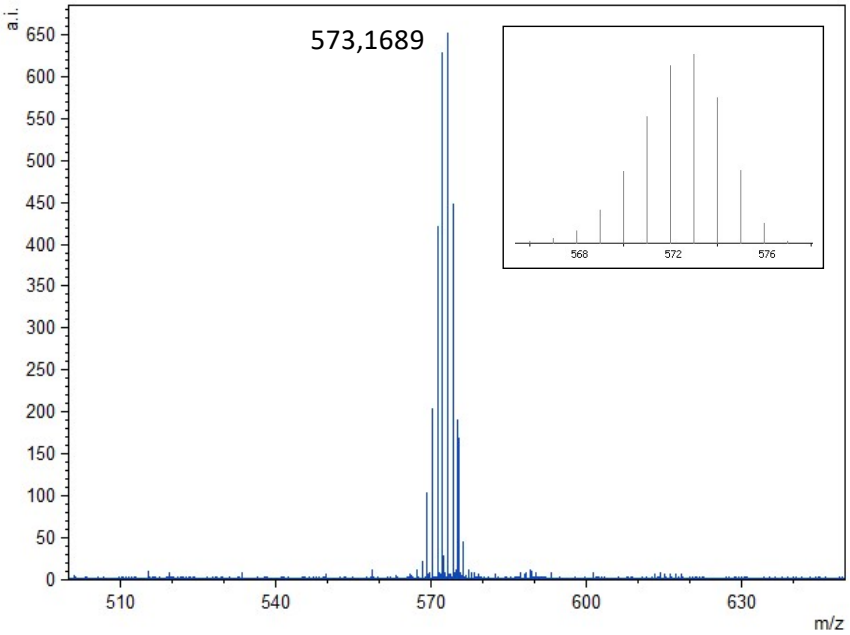

Figure S20. $^{1}H\{^{11}B\}$ NMR of Cs[**4**] in CD_3COCD_3.

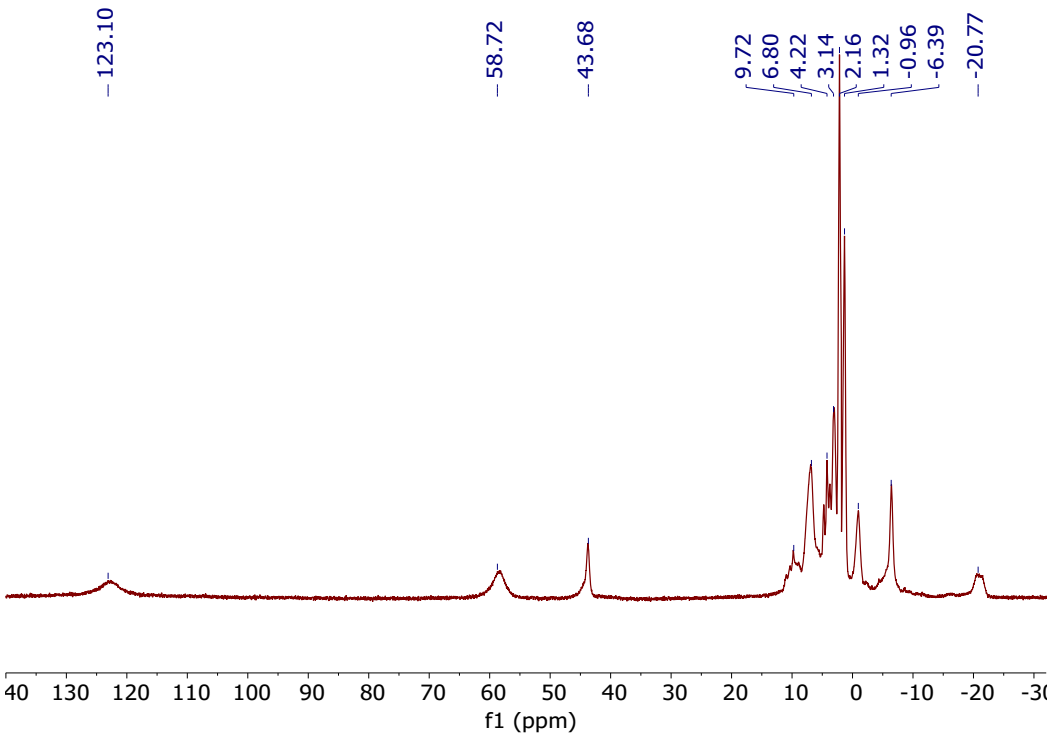

Figure S21. ^{1}H NMR of Cs[**4**] in CD_3COCD_3.

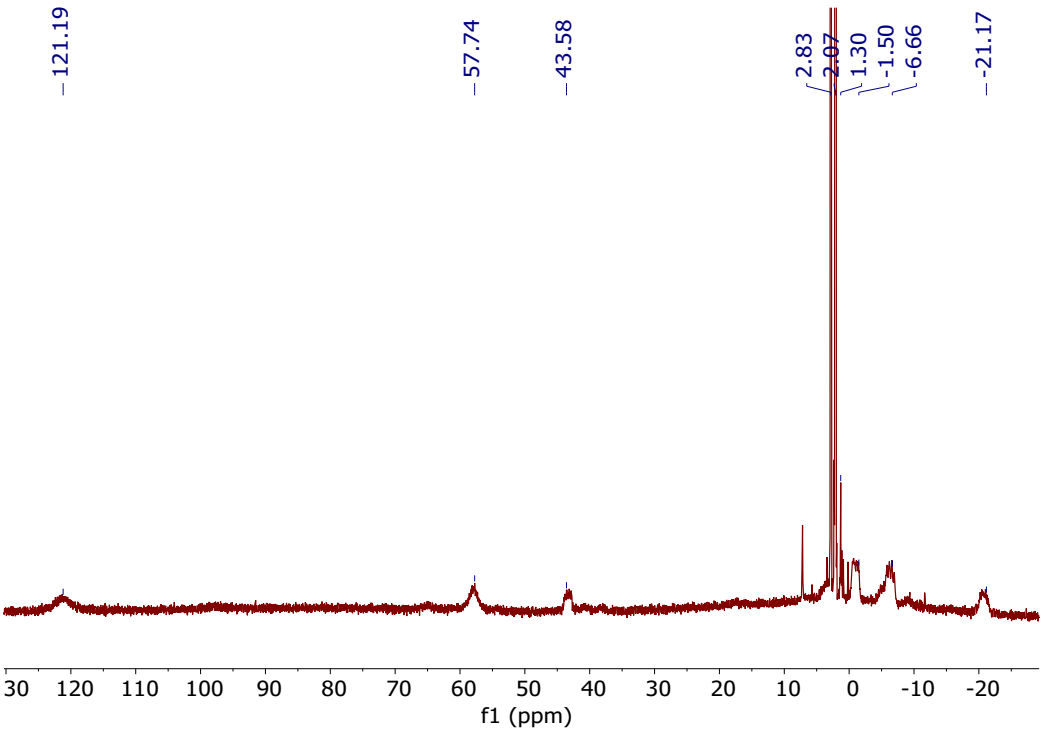

Figure S22. $^{11}B\{^{1}H\}$ NMR of Cs[**4**] in CD_3COCD_3.

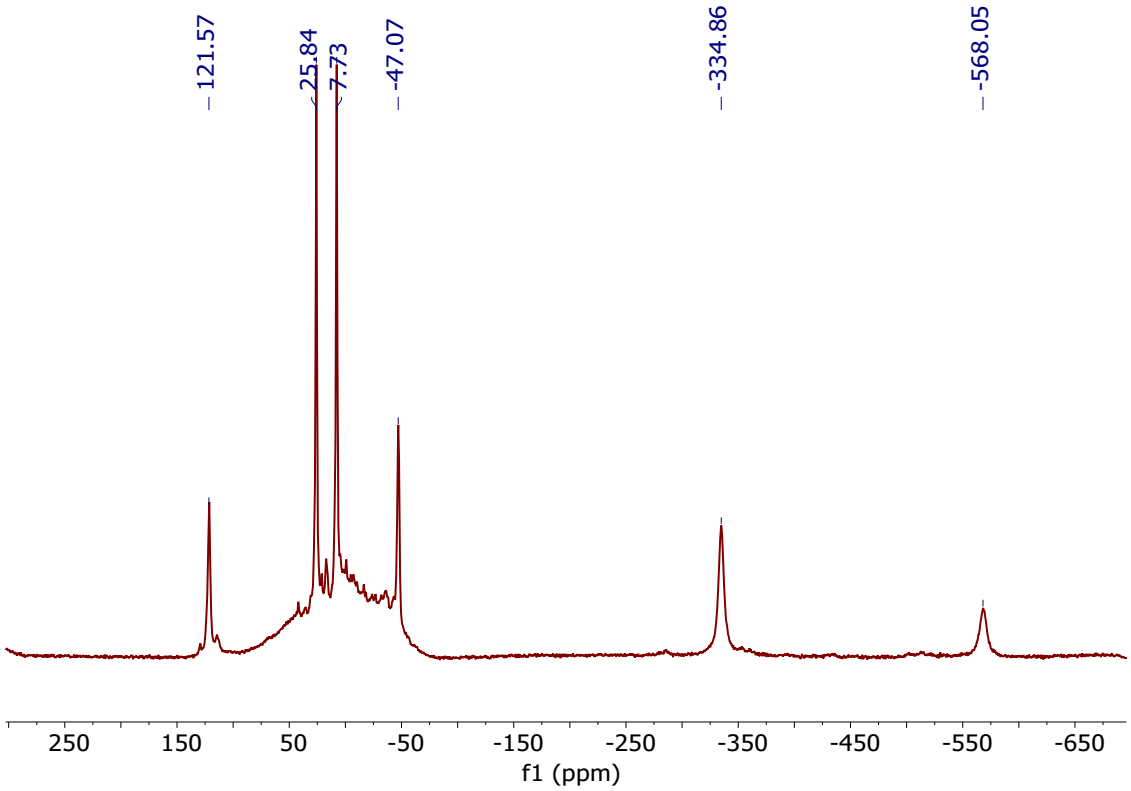

Figure S23. ^{11}B NMR of Cs[**4**] in CD_3COCD_3.

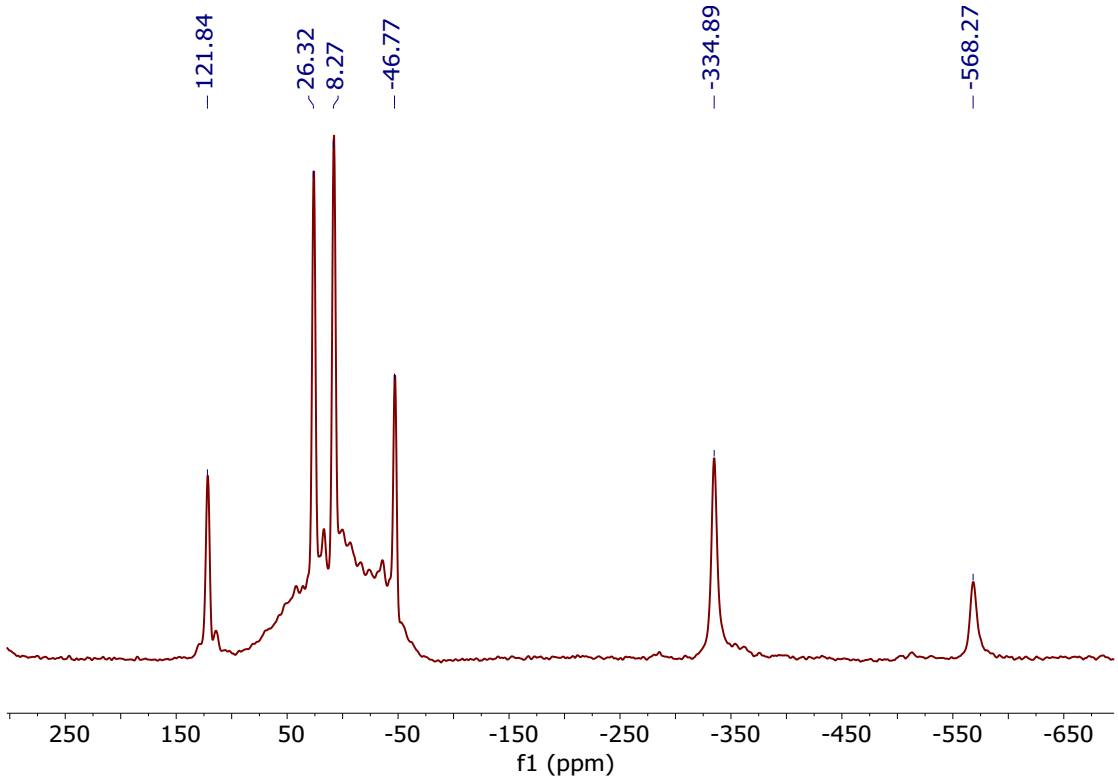

Characterization of Na[3,3'-Fe(8-I-1,2-$C_2B_9H_{11}$)$_2$]·2.5H_2O, abbreviated as Na[4].

Figure S24. IR spectra of Na[**4**].

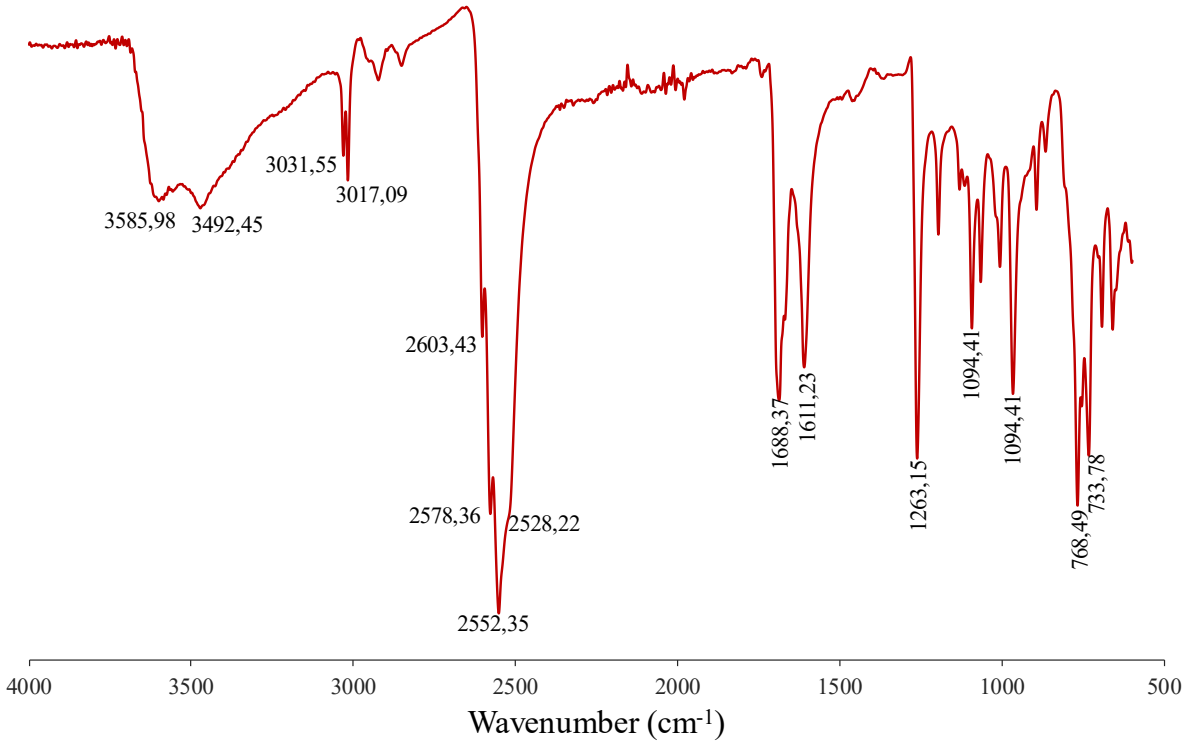

Figure S25. MALDI-TOF-MS experimental spectrum of Na[**4**]. Inset the theoretical MS.

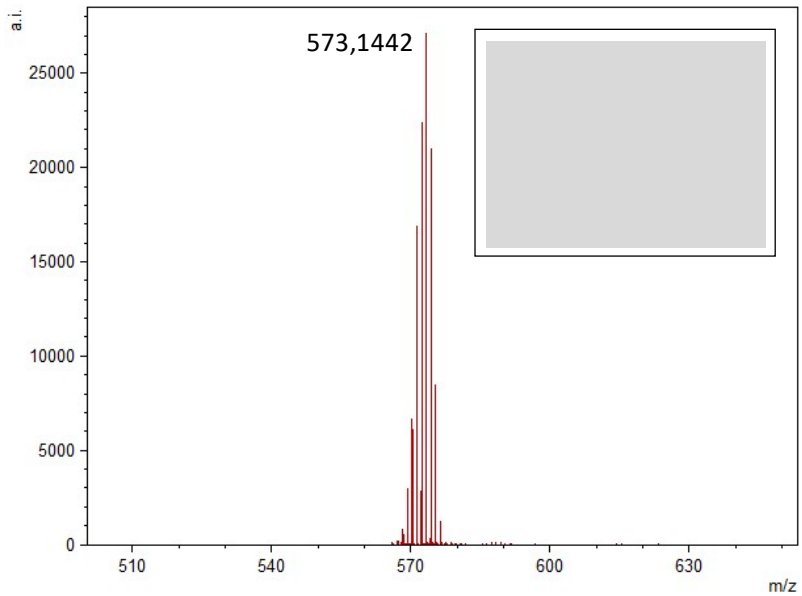

Figure S26. $^{1}H\{^{11}B\}$ NMR of Na[**4**] in CD_3COCD_3.

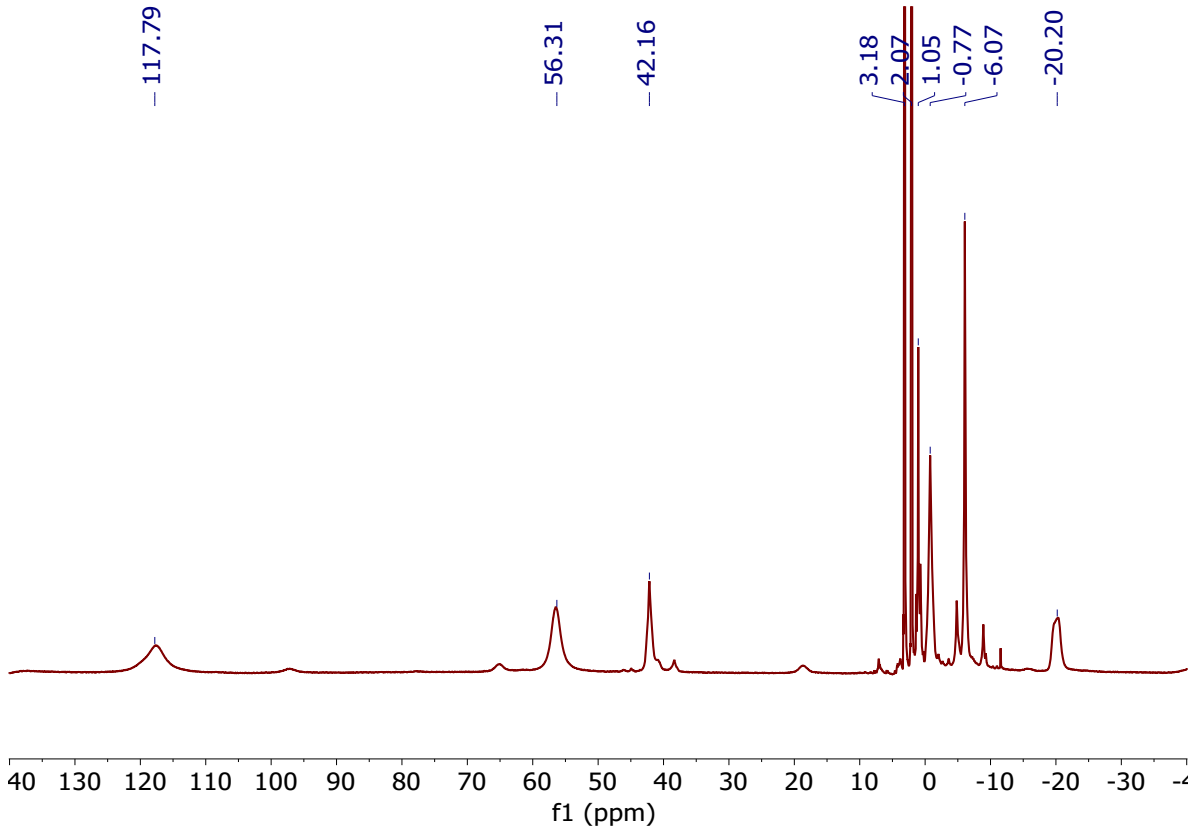

Figure S27. ^{1}H NMR of Na[**4**] in CD_3COCD_3.

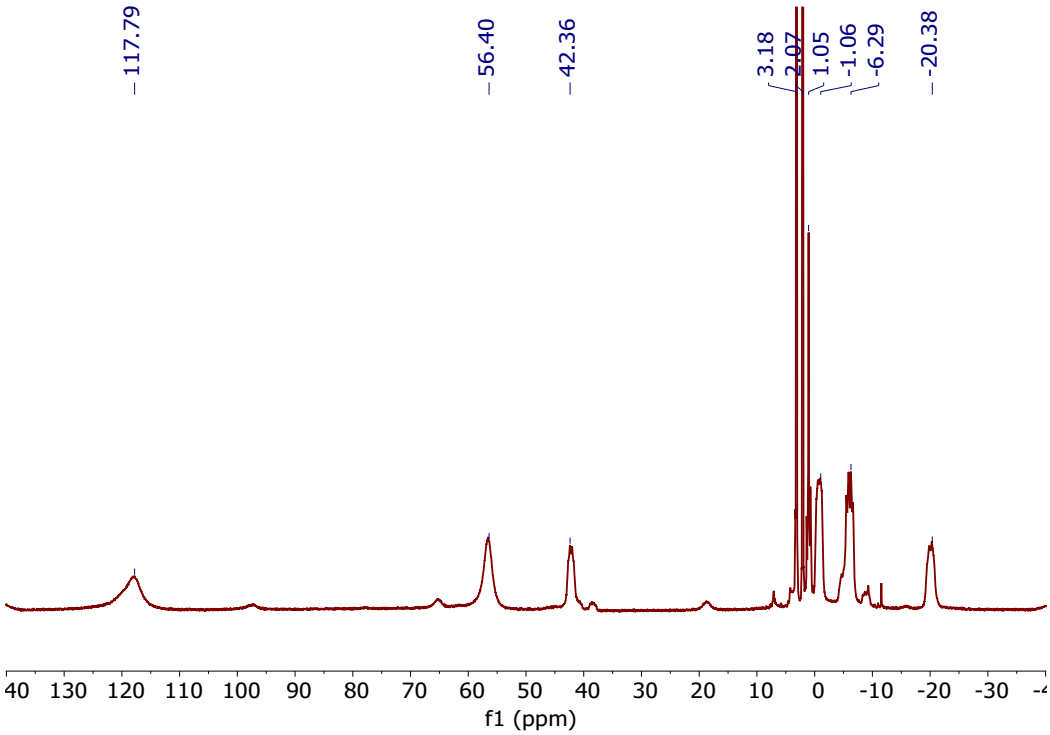

Figure S28. $^{11}B\{^{1}H\}$ NMR of Na[**4**] in CD_3COCD_3.

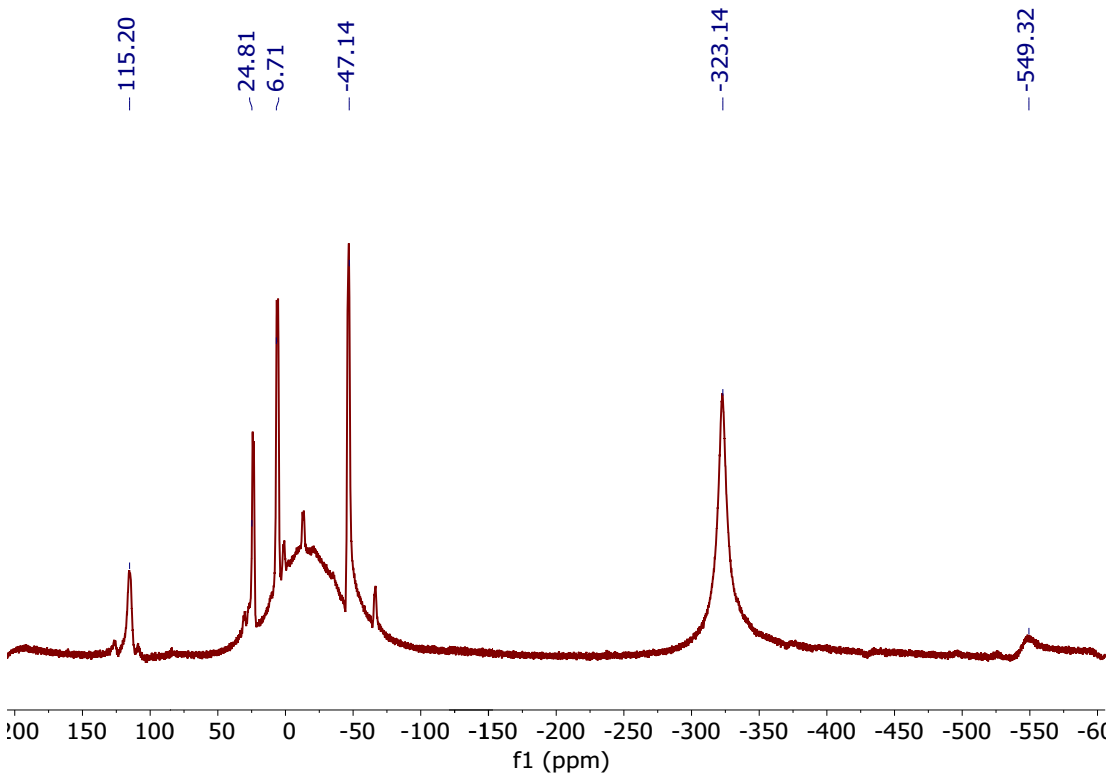

Figure S29. ^{11}B NMR of Na[**4**] in CD_3COCD_3.

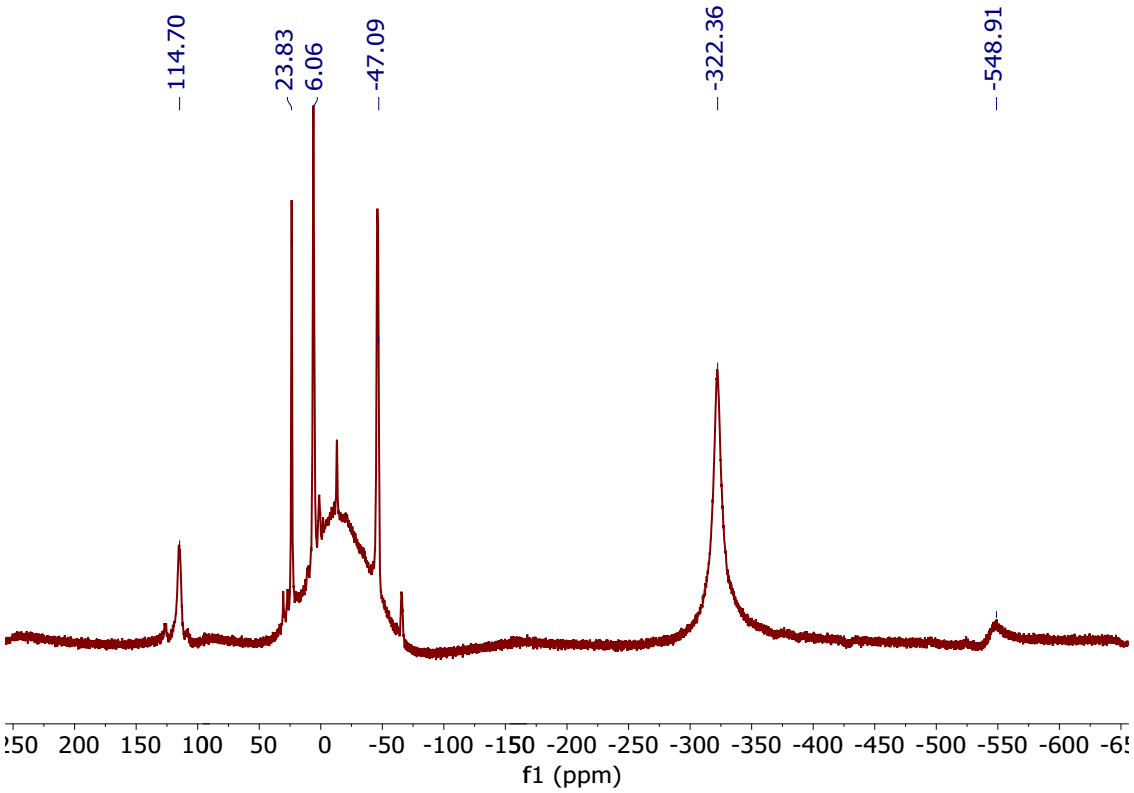

Figure S30. TGA/DSC spectra of Na[**4**].

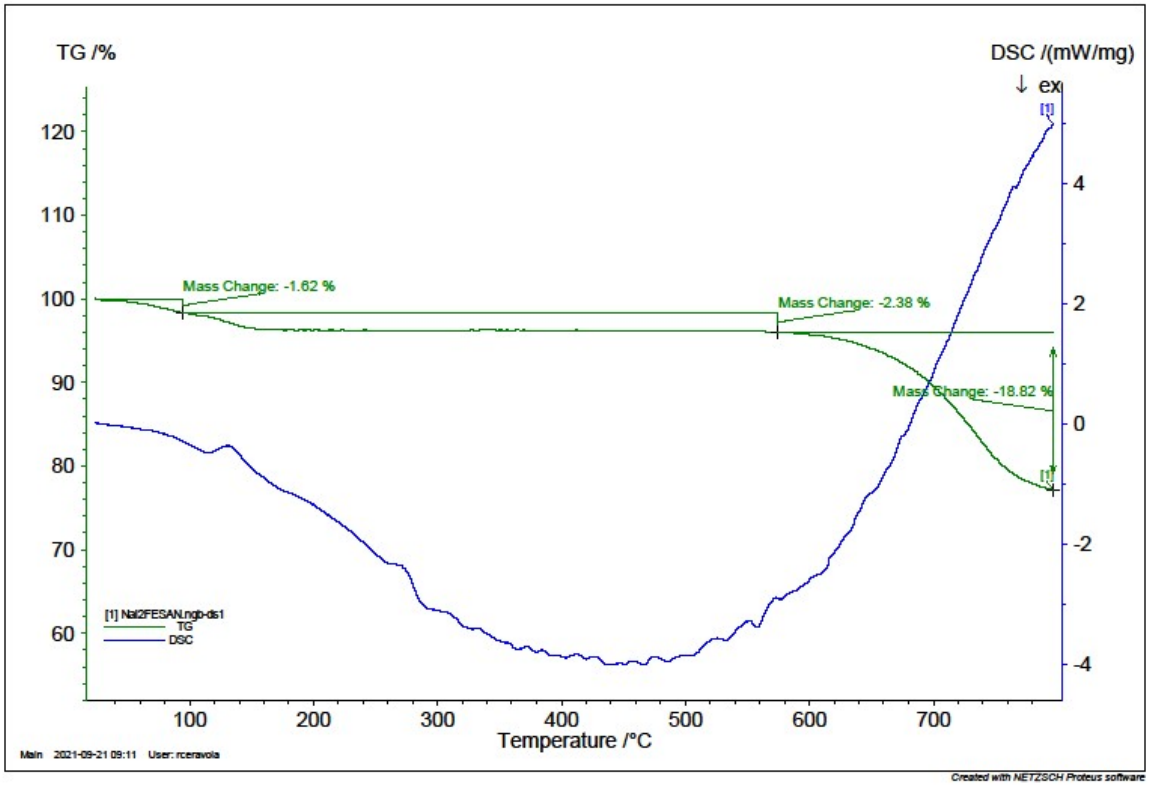

Figure S31. a) ^{11}B-NMR spectra of Na[**6**] in D_2O with the chemical shift numbers of the Boron vertices B(6), B(9,12), B(5,11), B(10), B(4,7) and B(8) from down to high field. b) ^{1}H-NMR spectra of Na[**6**] in D_2O.

a)

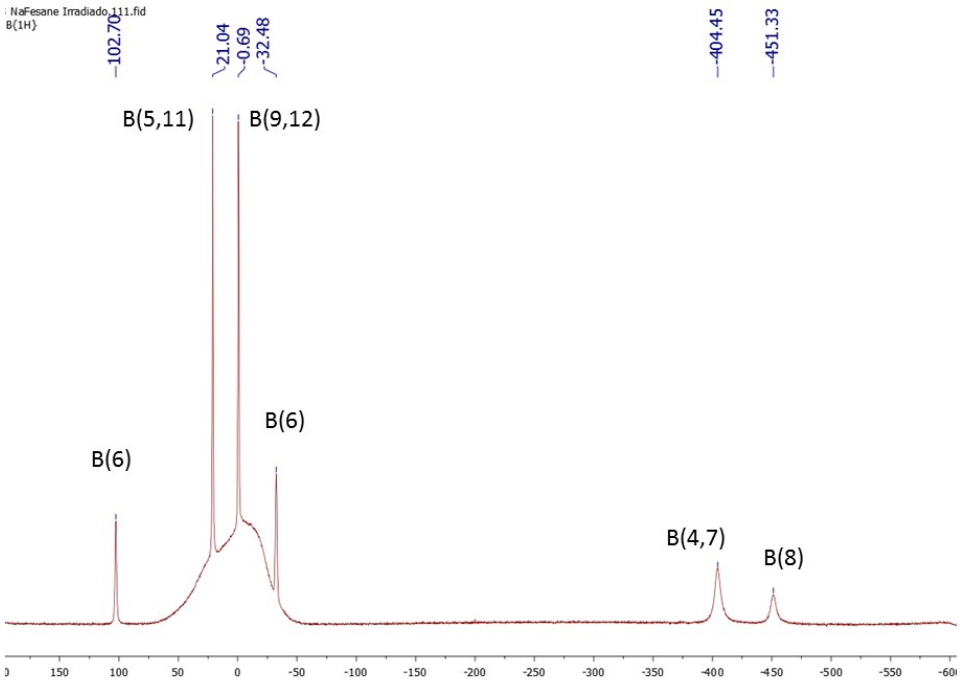

b)

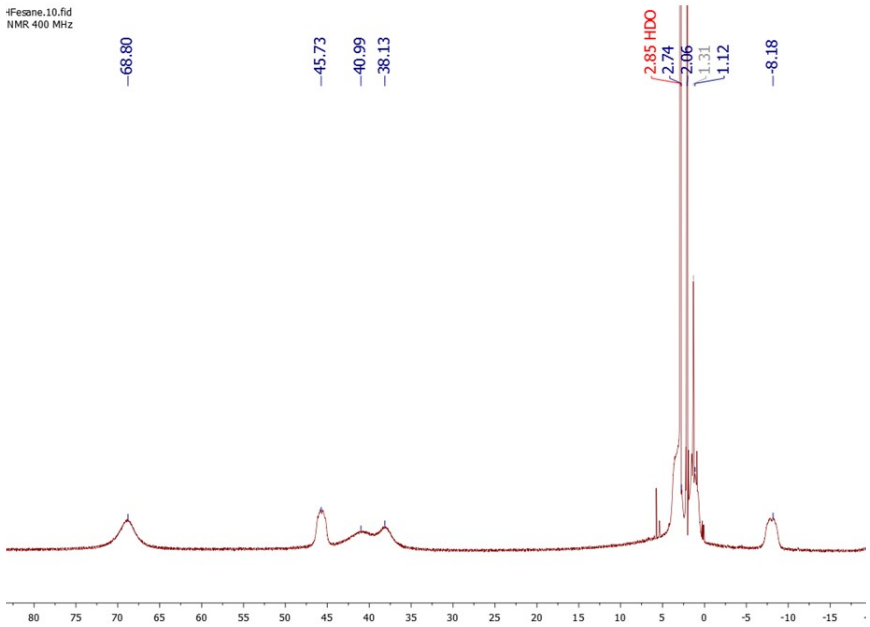

Figure S32. $^{11}B\{^{1}H\}$-NMR spectra of Na[**6**] in D_2O in the concentration range of 5-100 mM.

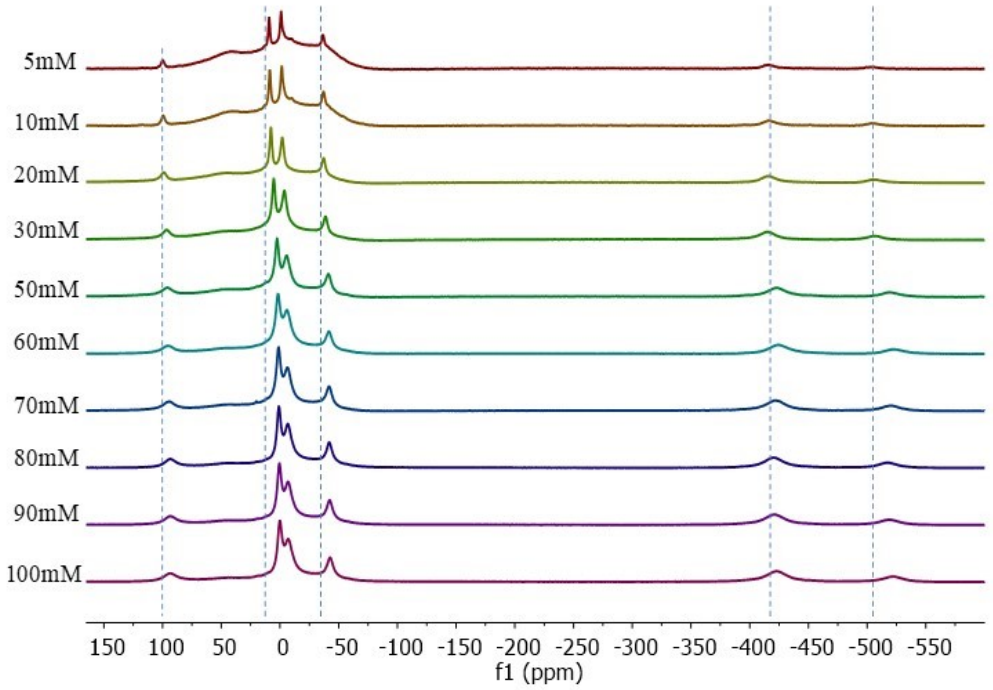

Figure S33. $^{1}H\{^{11}B\}$-NMR spectra of Na[**5**] in D_2O at different concentrations.

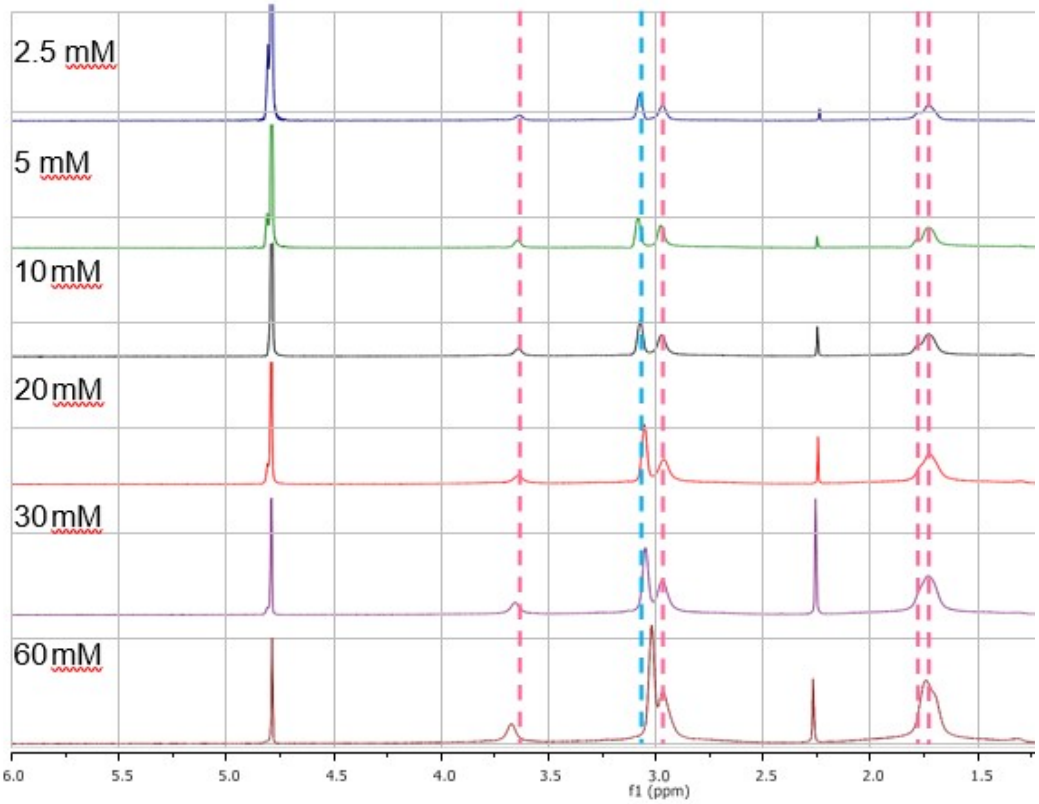

Figure S34. $^{11}B\{^{1}H\}$ NMR spectra of Na[**5**] in D_2O at different concentrations.

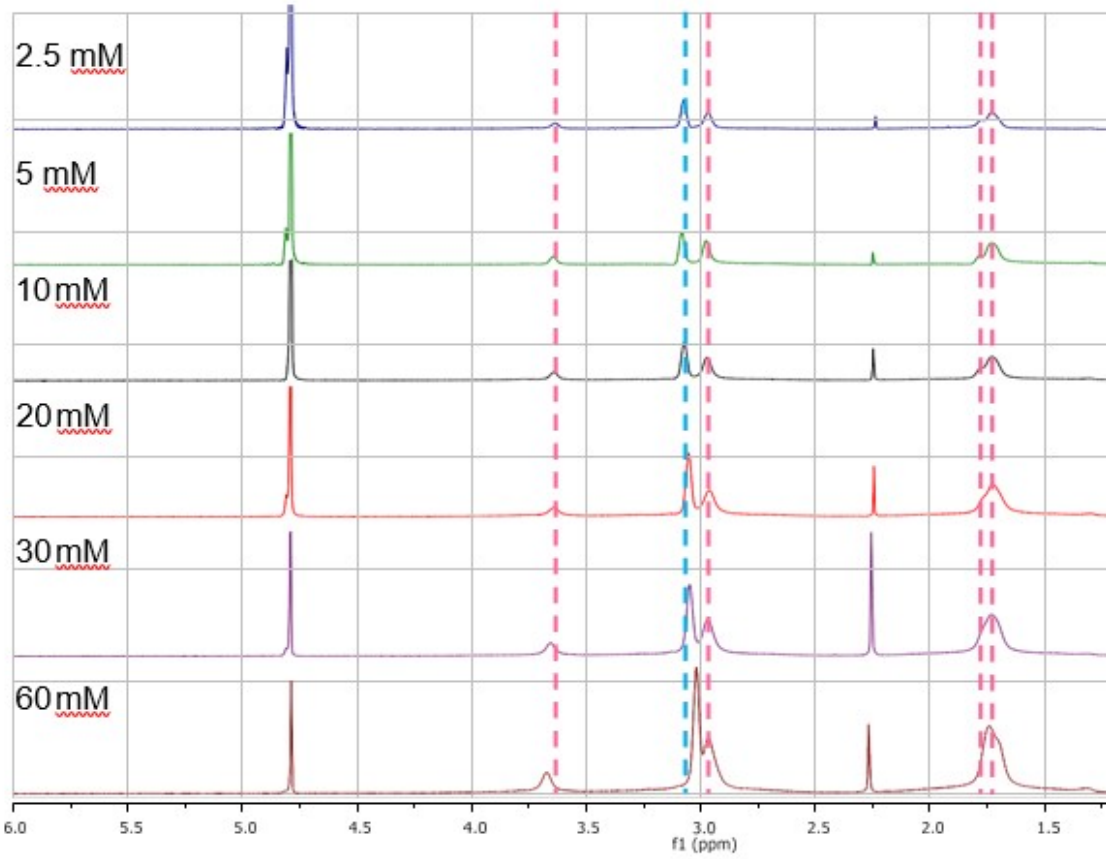

Table S1. Crystal data and structure refinement for $[(H_3O)(H_2O)_5][2,2'\text{-}Co(1,7\text{-}C_2B_9H_{11})_2]$, H[**5**], and $Cs(MeCN)[8,8'\text{-}I_2\text{-}Fe(1,2\ C_2B_9H_{10})_2]$, Cs[**4**].

Compound	$[(H_3O)(H_2O)_5][2,2'\text{-}Co(1,7\text{-}C_2B_9H_{11})_2]$	$Cs(MeCN)[8,8'\text{-}I_2\text{-}Fe(1,2\ C_2B_9H_{10})_2]$
Empirical formula	$C_4H_{35}B_{18}CoO_6$	$C_6H_{23}B_{18}CsFeI_2N$
Formula weight	432.83	746.39
Crystal system	Monoclinic	Monoclinic
Space group	C2/m	C2/c
a (Å)	8.0526(3)	21.9678(7)
b (Å)	11.2324(5)	12.5135(4)
c (Å)	12.1312(6)	8.9201(3)
□□(º)	90	90
□□(º)	103.702(2)	105.4220(10)
□□(º)	90	90
V(Å^3)	1066.04(8)	2363.79(13)
Z	2	4
F(000)	448	1372
Theta range for data collection	3.17 to 27.50°	2.198 to 29.470°
Reflections collected	26669	11149
Independent reflections	1284	2022 [R(int) = 0.0533]
Data / restraints / parameters	1284 / 0 / 80	2022 / 0 / 137
Goodness-of-fit on F^2	1.202	1.103
R1 (I>2□□I))	0.0273	0.0409
wR2 (I>2□(I))	0.0725	0.1347
R1 (all data)	0.0305	0.0433
wR2 (all data)	0.0752	0.1399

Cyclic voltammetry studies.

Figure S35. The CV wave of Na[**1**] $E_{1/2}$ = -1.81V versus F_c^+/F_c.

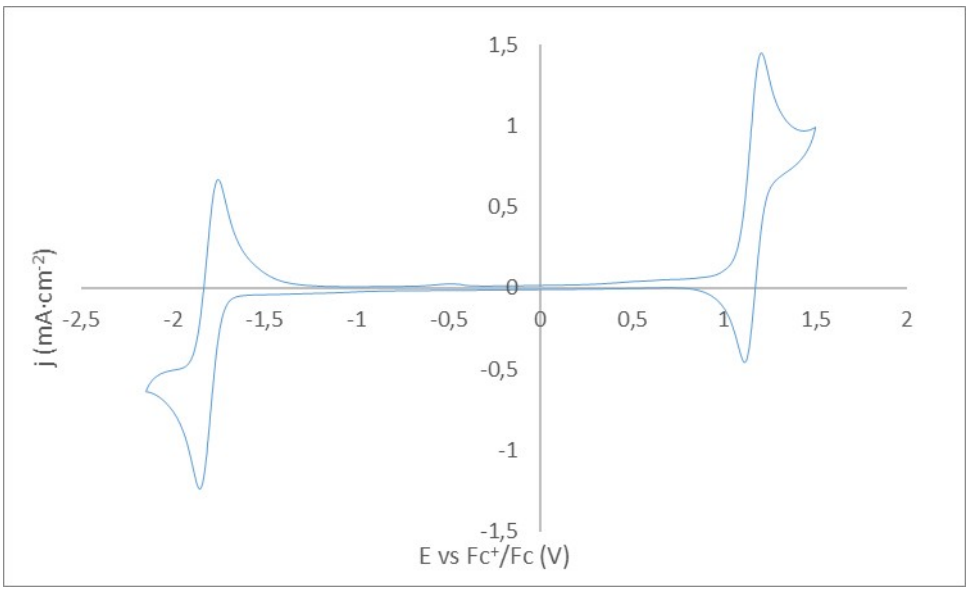

Figure S36. The CV wave of Na[**2**]. $E_{1/2}$ = -0.73V versus F_c^+/F_c.

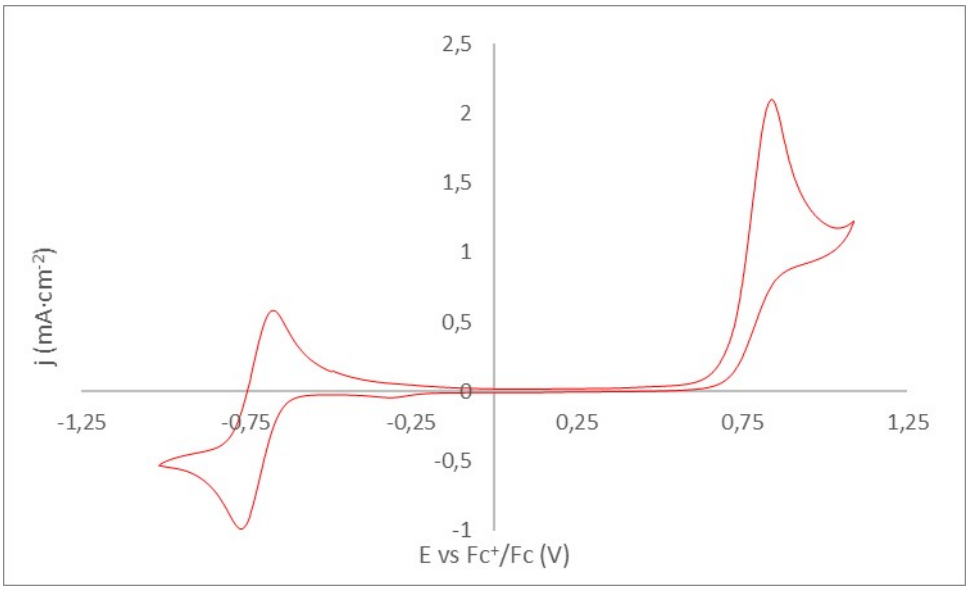

Figure S37. The CV wave of Na[**3**]. $E_{1/2}$ = -1.33V versus F_c^+/F_c.

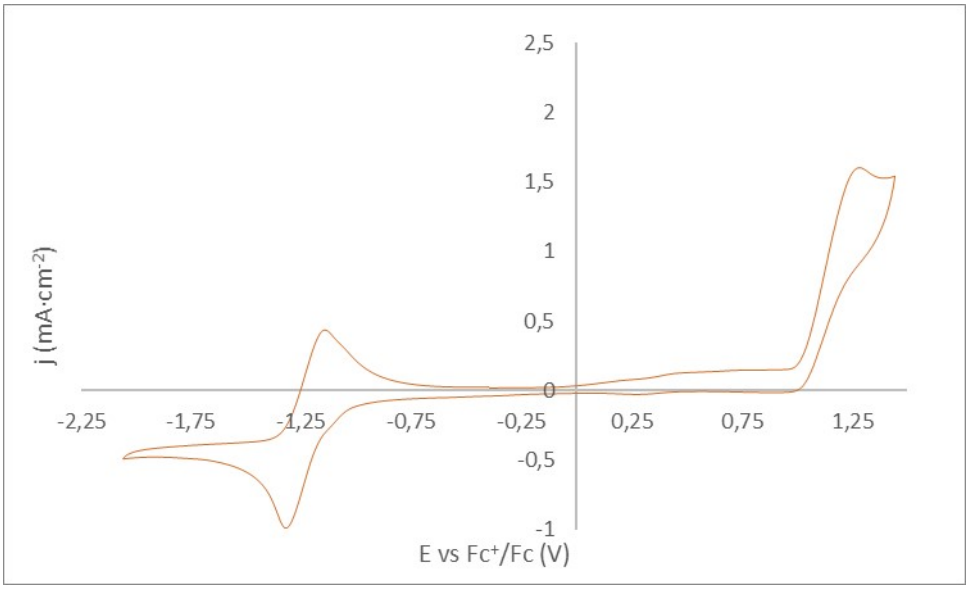

Figure S38. The CV wave of Na[**4**] such as $E_{1/2}$ = -0.36 V versus F_c^+/F_c.

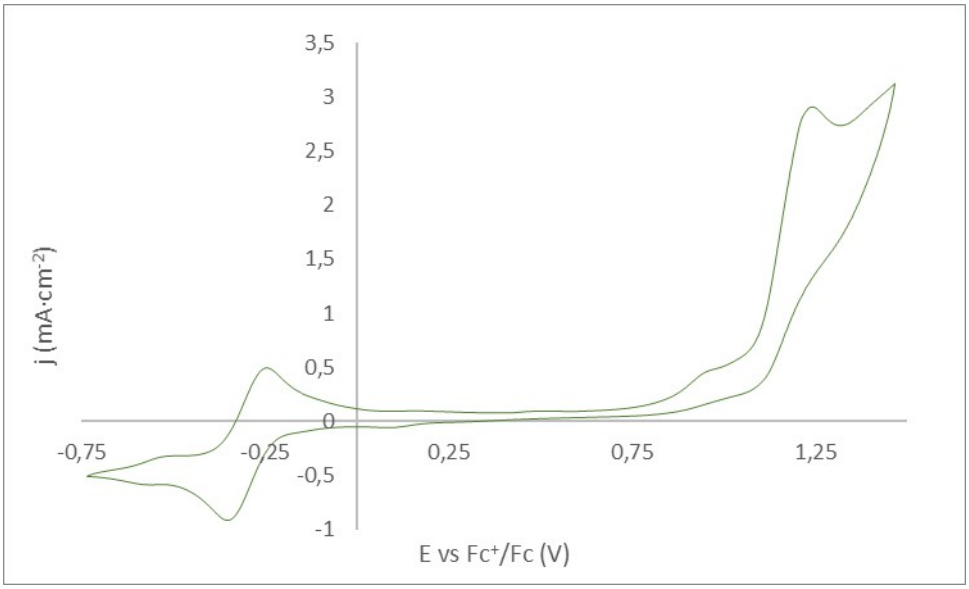

Figure S39. The CV wave of Na[**5**]. $E_{1/2}$ = -1.55 V versus F_c^+/F_c.

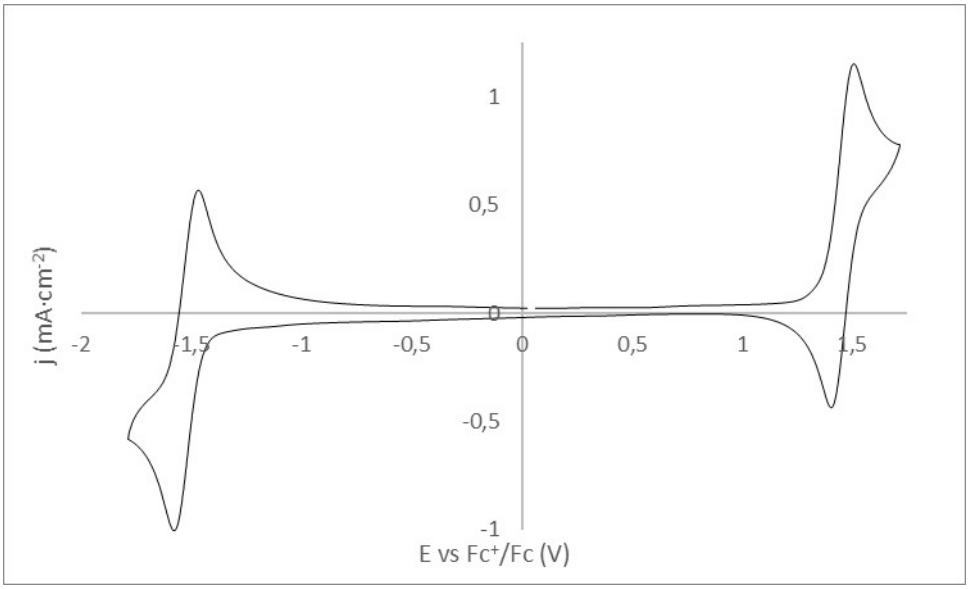

Figure S40. The CV wave of Na[**6**]. $E_{1/2}$ = -0.79 V versus F_c^+/F_c.

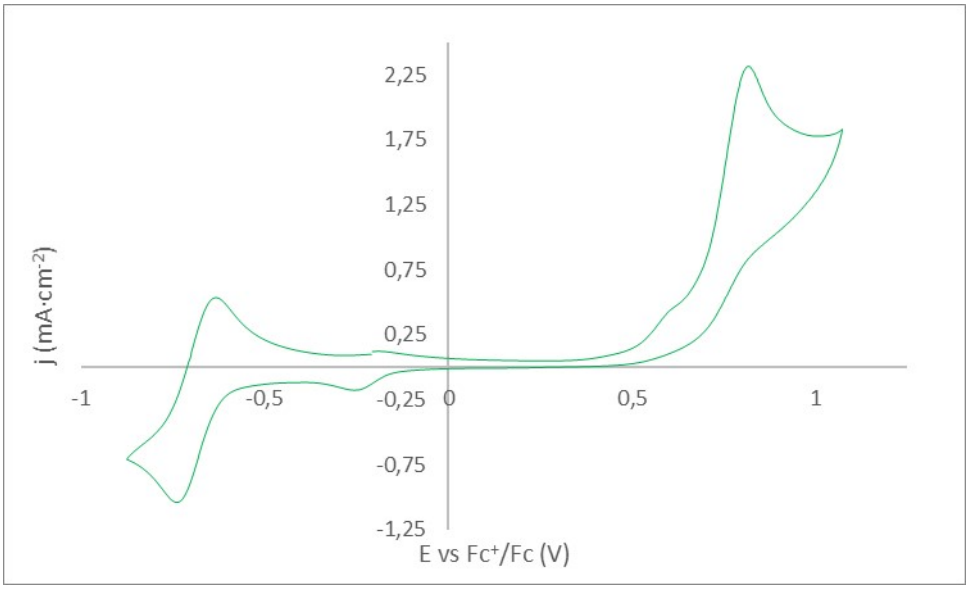

Figure S41. Electrolysis behavior of [**6**]$^{-}$.

On the left (brown): natural state (Fe^{3+}, d^5); on the right (pink): reduced state (Fe^{2+} d^6).

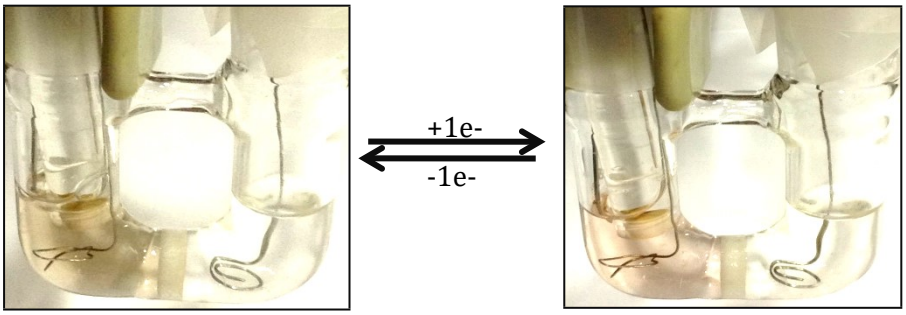

Solubility studies.

Figure S42. Solubility study of Na[3,3'-Fe(1,2-$C_2B_9H_{11})_2$], Na[**1**] in H_2O; Plot of absorbance *vs.* concentration.

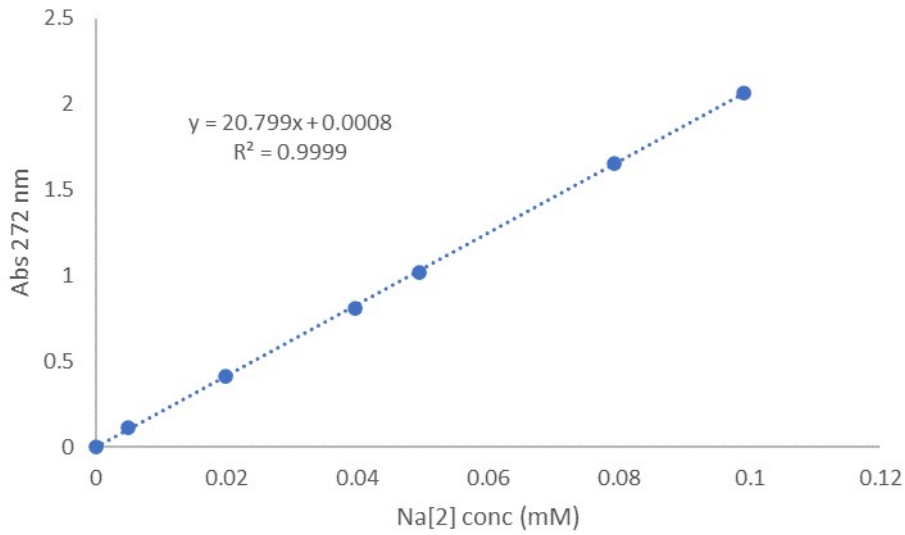

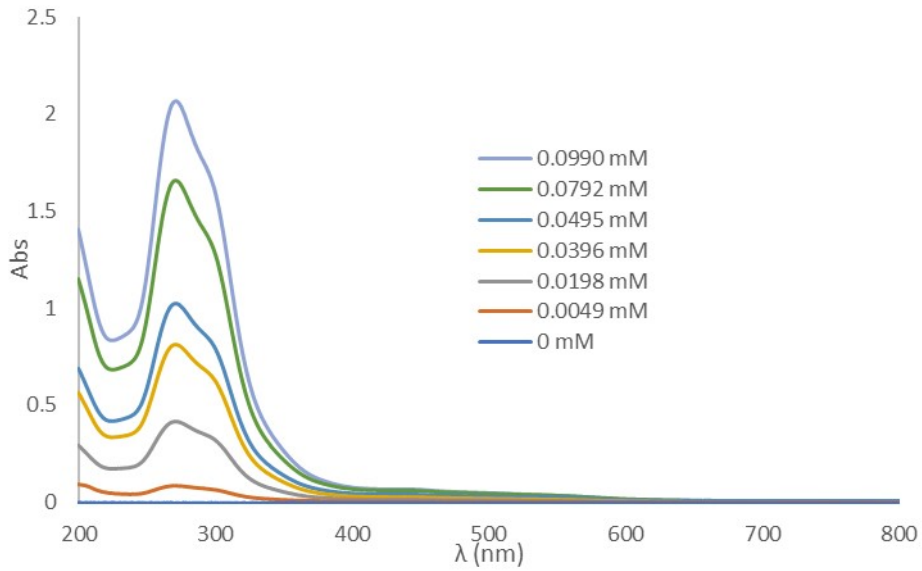

Solubility of Na[**2**] in water 1.247±0.018 M or 484.72±7.01 g/L

Figure S43. Solubility study of Na[**4**] in water; Plot of absorbance *vs.* concentration

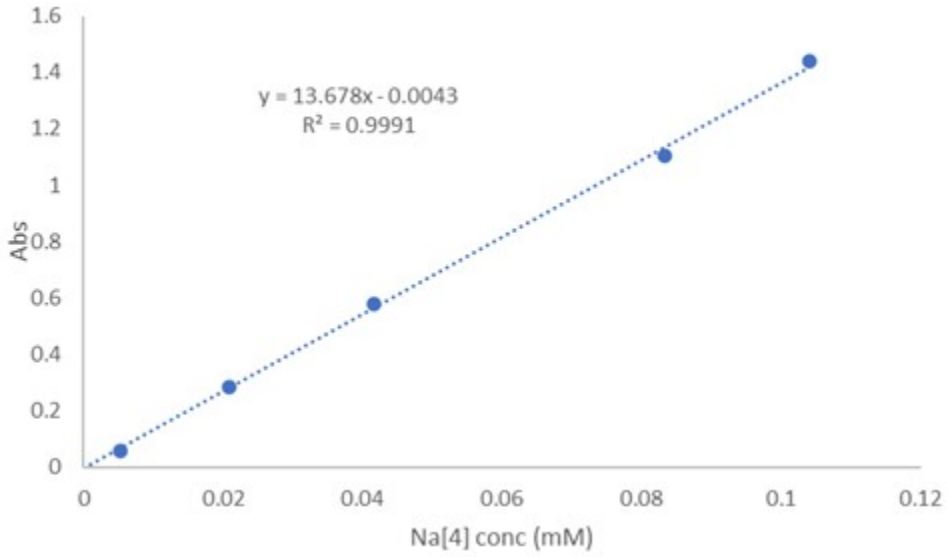

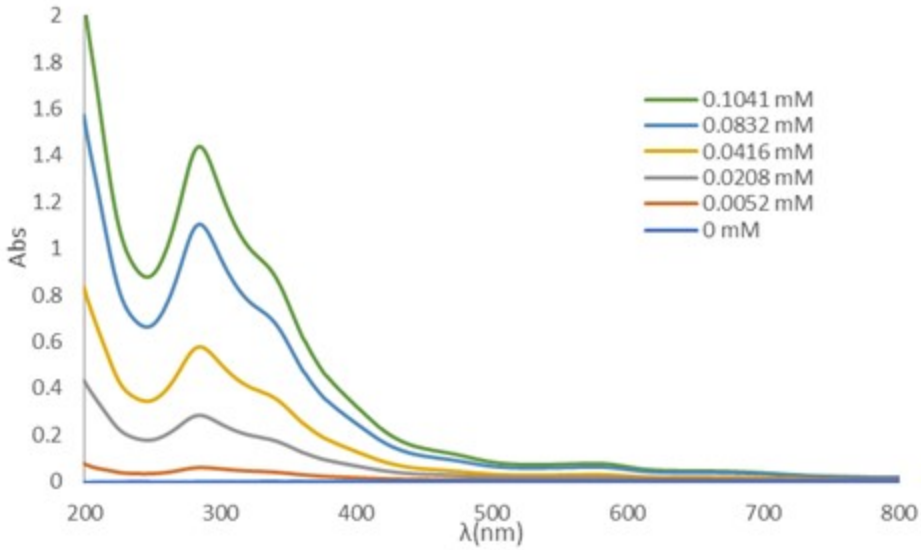

Solubility of Na[**4**] in water 0.374±0.006 M or 240.14±3.80 g/L

Figure S44. Solubility study of Na[**5**] in H_2O. Plot of absorbance *vs.* concentration

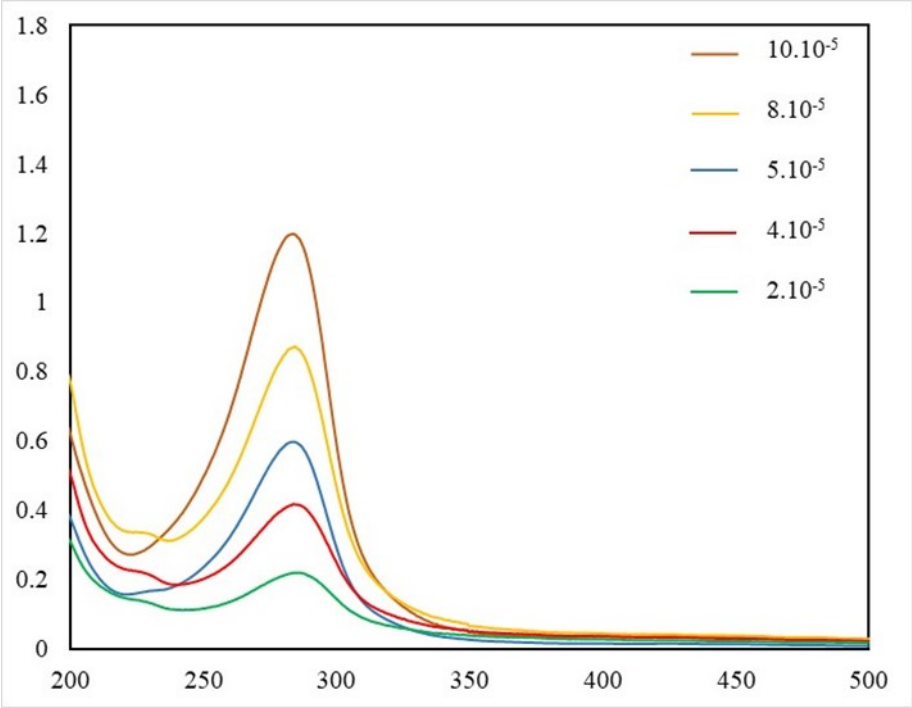

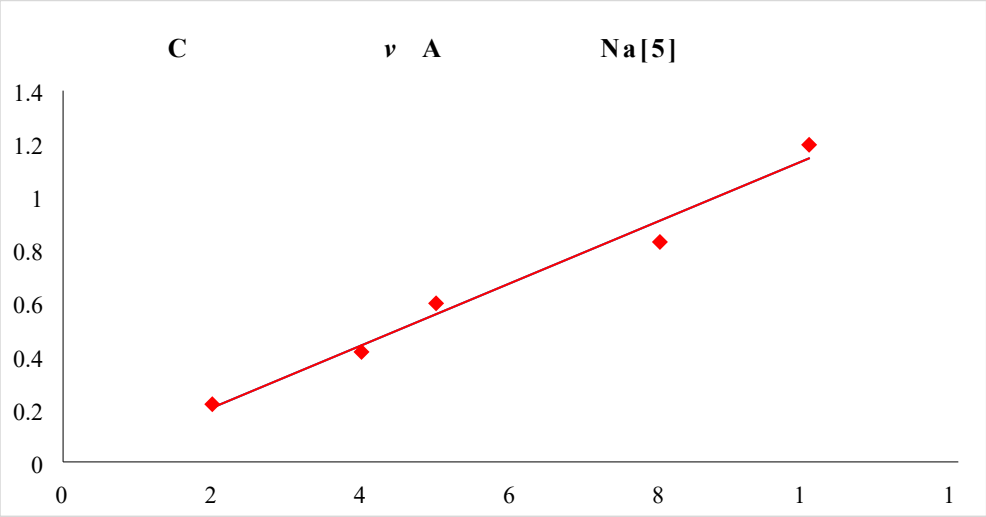

Solubility of Na[**5**]= 1726 mM.

Figure S45. Solubility study of Na[**6**] in H_2O. Plot of absorbance *vs.* concentration.

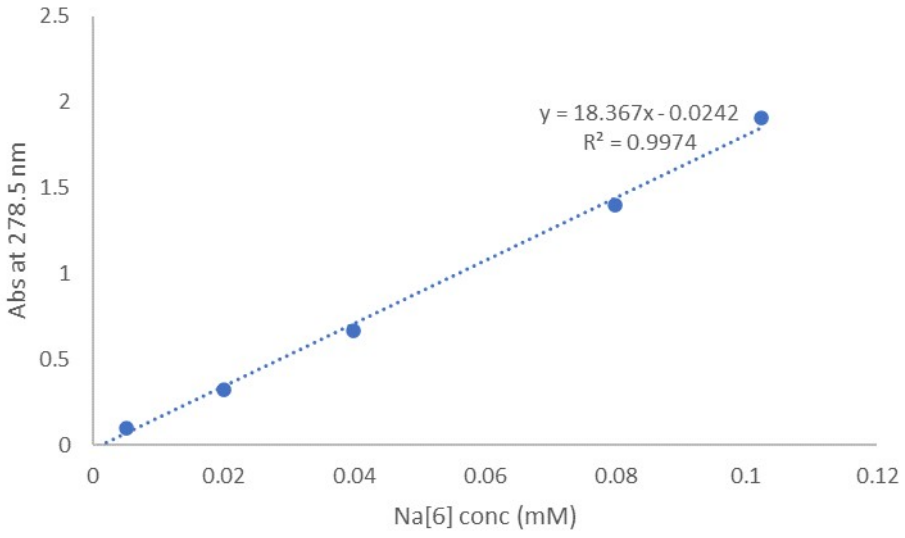

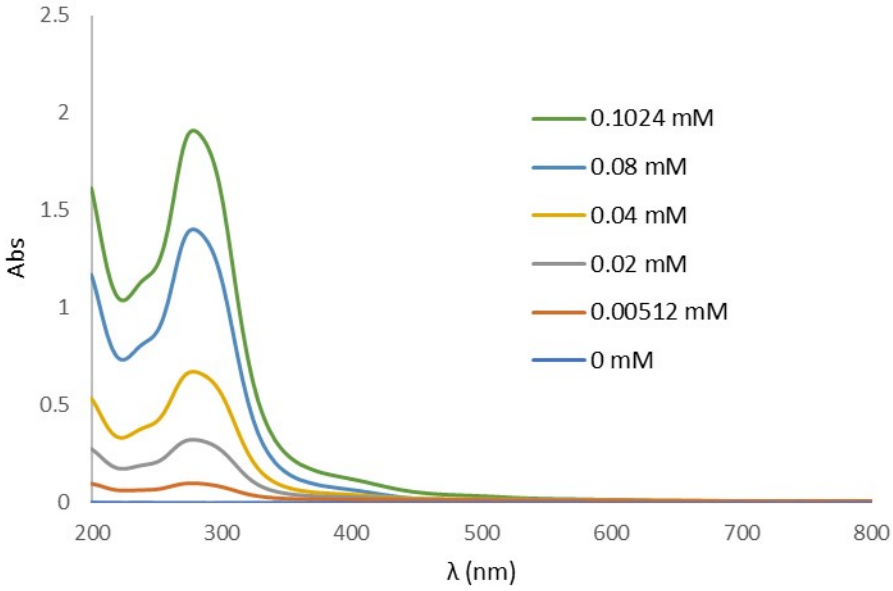

Solubility of Na[**6**] in water 1.400±0.025 M or 544.56±9.86 g/L

Lipophilicity Studies.

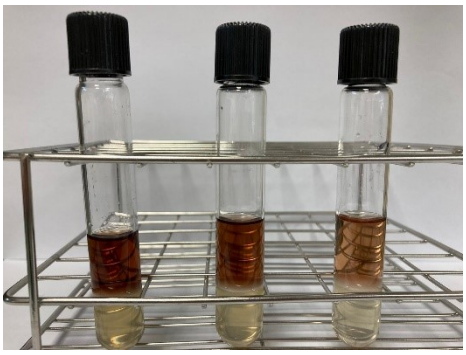

Figure S46. Lipophilicity of Na[**5**].

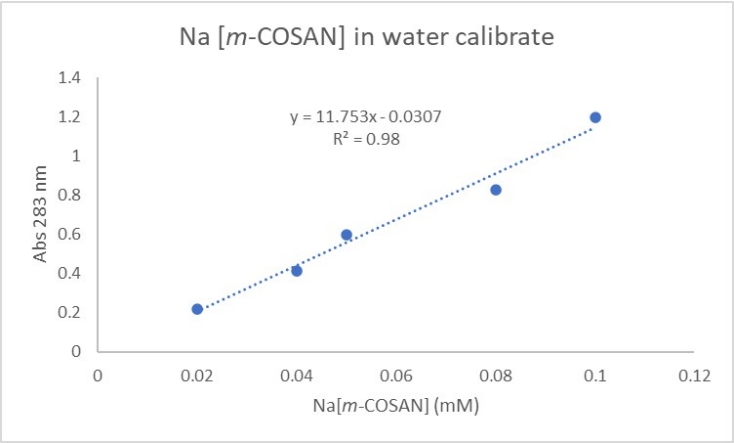

Sample	Amount of Na[mCOSAN]	Na[mCOSAN] concentration in 1-octanol	Na[mCOSAN] concentration in water	P	Log P
1	1.27 mg	1.04 mM	0.037 mM	27.94	1.44
2	3.27 mg	2.48 mM	0.296 mM	8.37	0.92
3	4.95 mg	4.04 mM	0.167 mM	24.16	1.38
4	2.72 mg	2.22 mM	0.076 mM	29.17	1.46
5	2.74 mg	2.20 mM	0.095 mM	23.07	1.36

Average P	Average log P
26.09±2.92	1.41±0.05

Figure S47. Lipophilicity of Na[**2**]

Sample	Amount of Na[FESAN]	Na[FESAN] concentration in 1-octanol	Na[FESAN] concentration in water	P	Log P
1	3.104 mg	3.074 mM	0.077 mM	39.44	1.59
2	2.956 mg	2.99 mM	0.063 mM	47.20	1.67
3	5.624 mg	5.61 mM	0.108 mM	50.48	1.70

Average P	Average log P
45.70±5.66	1.65±0.05

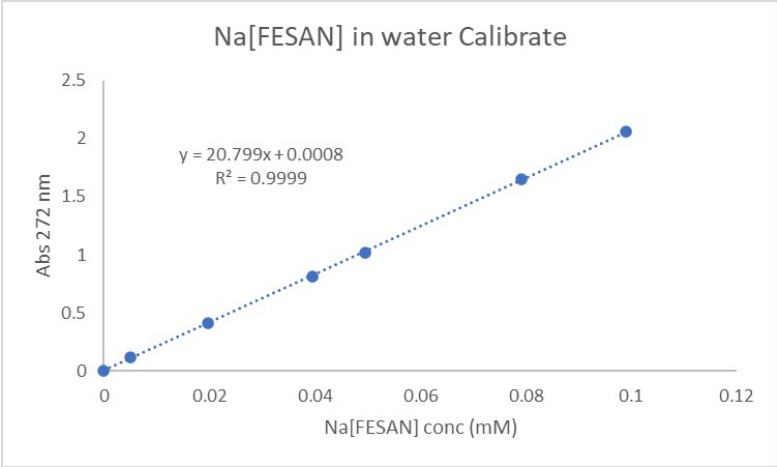

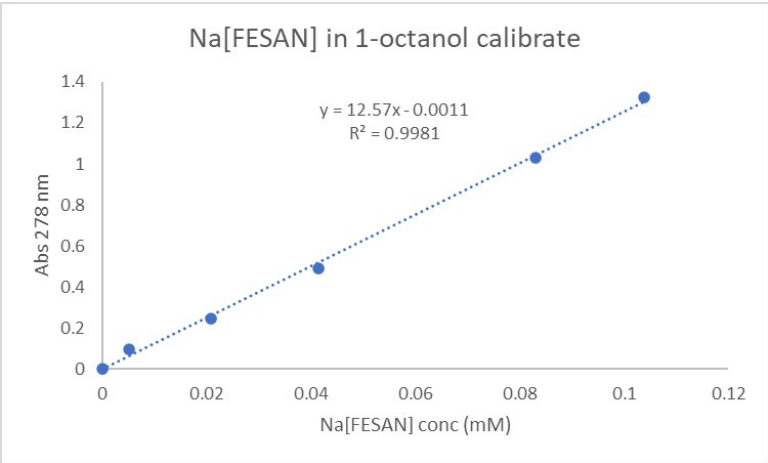

Figure S48. Lipophilicity of Na[**4**]

Sample	Amount of Na[I_2-FESAN]	Na[I_2-FESAN] concentration in 1-octanol	Na[I_2-FESAN] concentration in water	P	Log P
1	5.92 mg	3.66 mM	0.041 mM	89.08	1.949
2	4.21 mg	1.84 mM	0.017 mM	103.94	2.016
3	4.56 mg	2.14 mM	0.020 mM	104.90	2.021

Average P	Average log P
99.31±8.86	1.99±0.04

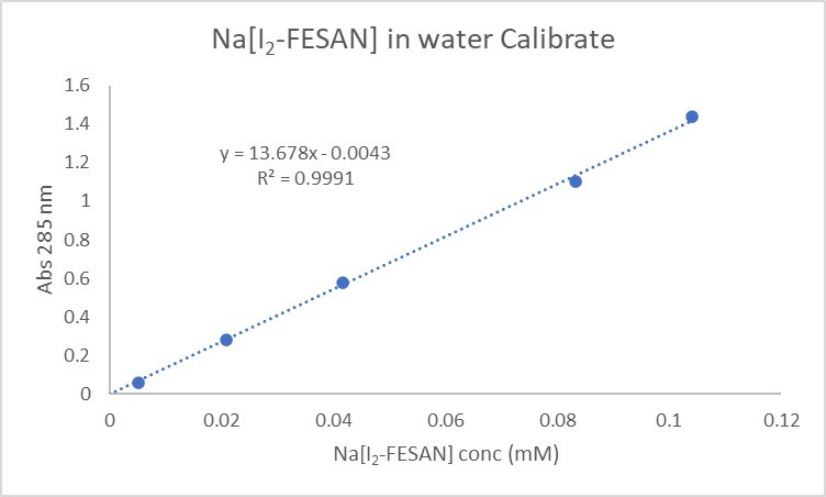

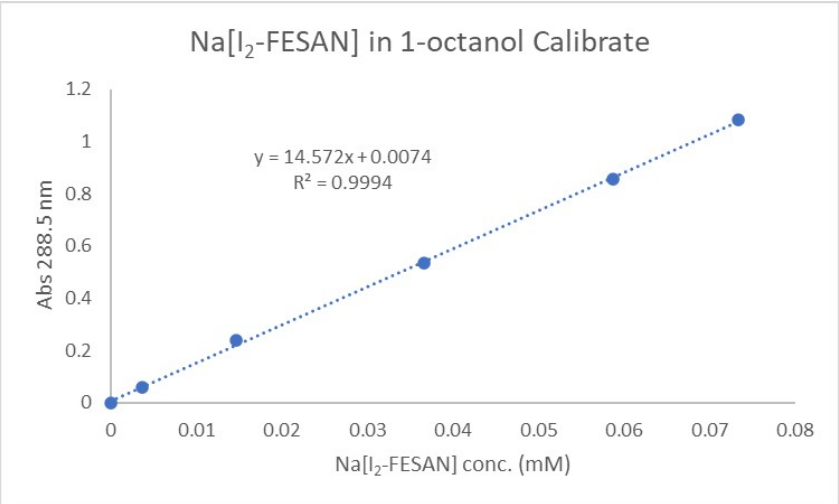

Figure S49. Lipophilicity of Na[**6**].

Sample	Amount of Na[*m*-FESAN]	Na[*m*-FESAN] concentration in 1-octanol	Na[*m*-FESAN] concentration in water	P	Log P
1	0.865 mg	1.34 mM	0.040 mM	33.27	1.52
2	1.327 mg	2.17 mM	0.061 mM	35.43	1.55
3	1.704 mg	2.67 mM	0.072 mM	37.03	1.57

Average P	Average log P
35.24±1.88	1.55±0.02

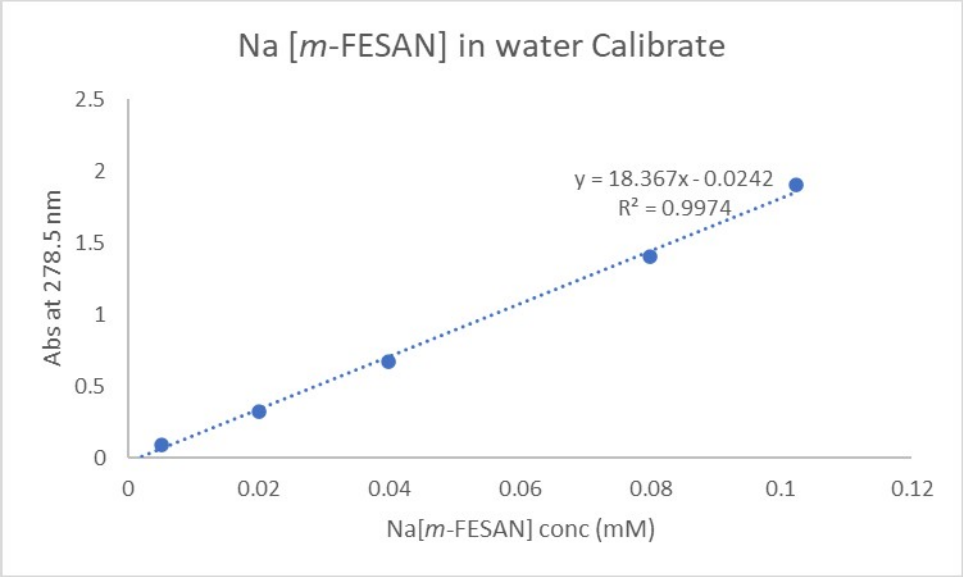

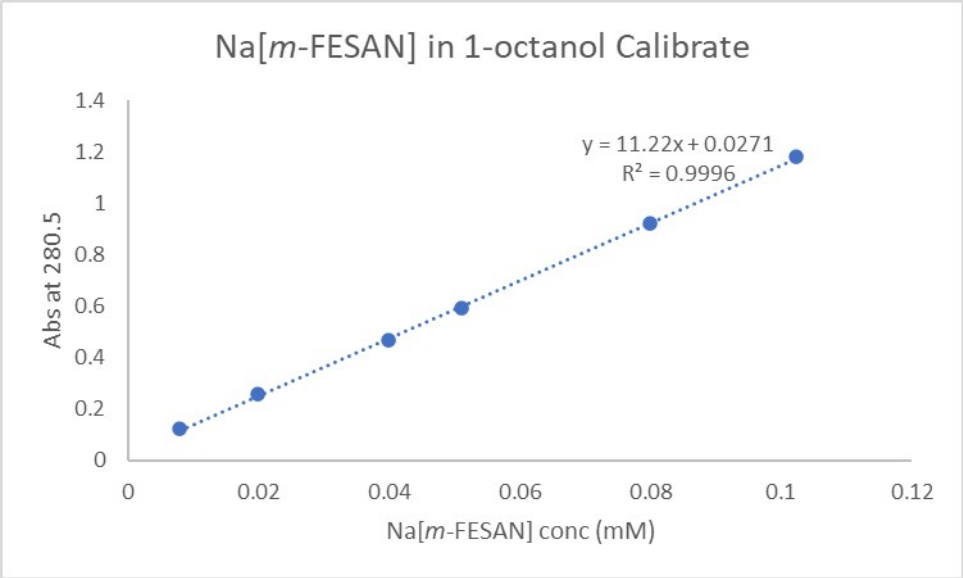

Figure S50. Dynamic lattice scattering of Na[**5**] in H_2O (a) Size distribution by Intensity and (b) Raw correlation data presentation

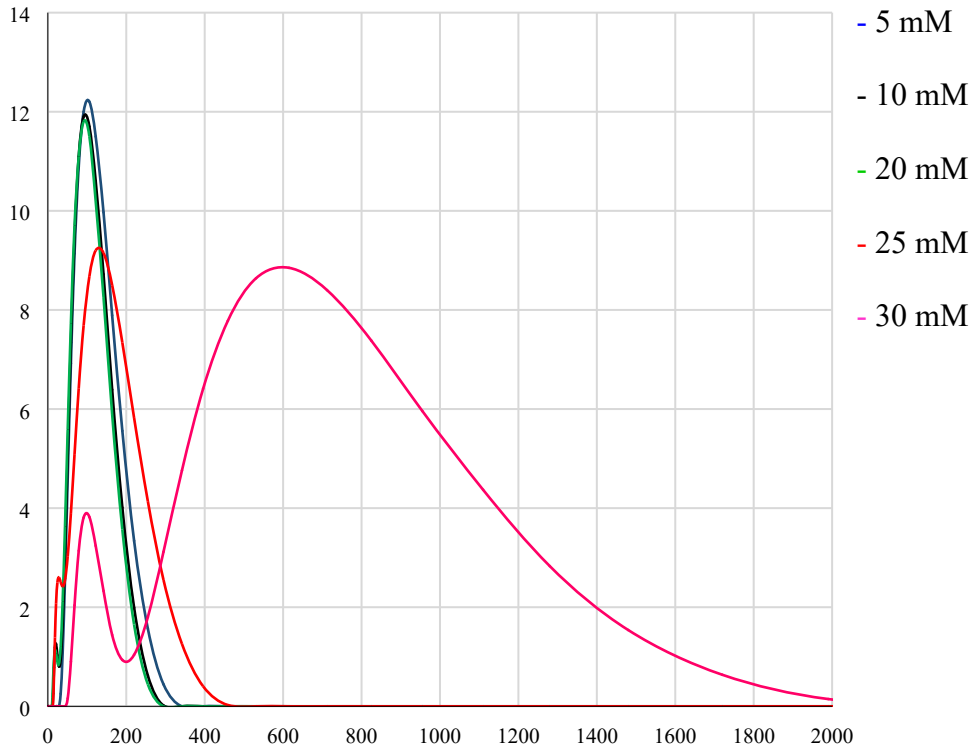

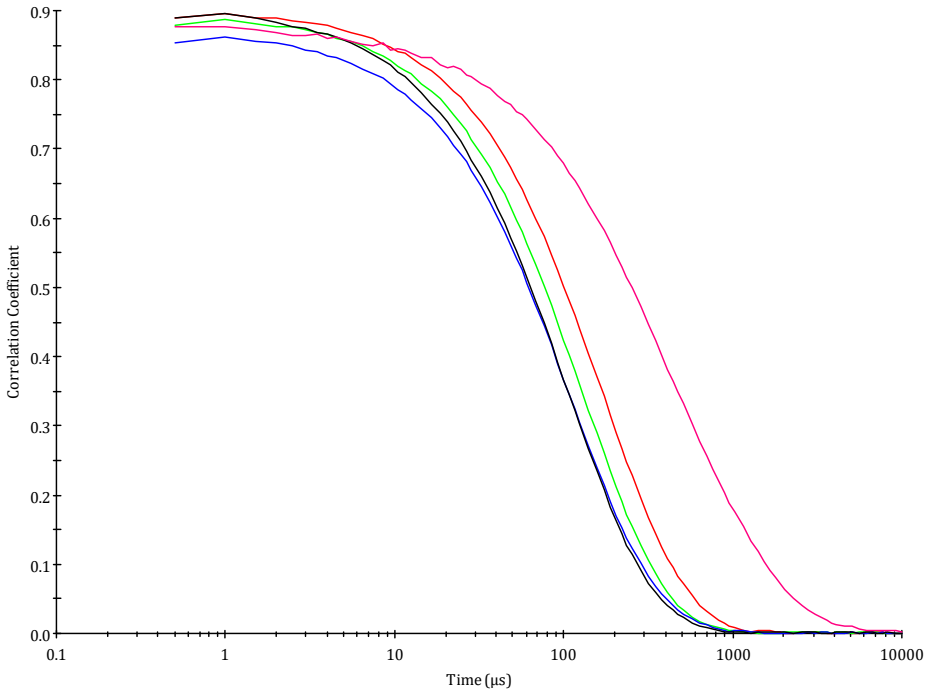

References

[1] a) M. F. Hawthorne, D. C. Young and P. A. Wegner, Carbametallic boron hydride derivatives. I. Apparent analogs of ferrocene and ferricinium ion, *J. Am. Chem. Soc*., 1965, **87**, 1818-1819. b) M. F. Hawthorne and T. D. Andrews, Carborane analogues of cobalticinium ion, *J. Chem. Soc., Chem. Comm.*, 1965, 443-444. c) M. F. Hawthorne, D. C. Young, T. D. Andrews, D. V. Howe, R. L. Pilling, A. D. Pitts, M. Reintjes, L. F. Warren, Jr and P. A. Wegner, pi.-Dicarbollyl derivatives of the transition metals. Metallocene analogs, *J. Am. Chem. Soc*., 1968, **90**, 879-896. d) C. Viñas, J. Pedrajas, J. Bertran, F. Teixidor, R. Kivekäs and R. Sillanpää, Synthesis of Cobaltabis(dicarbollyl) Complexes Incorporating Exocluster SR Substituents and the Improved Synthesis of [3,3‘-Co(1-R-2-R‘-1,2-C2B9H9)2]- Derivatives, *Inorg. Chem*., 1997, **36**, 2482-2486.

[2] a) R. A. Wiesboeck and M. F. Hawthorne, Dicarbaundecaborane(13) and Derivatives, *J. Am. Chem. Soc.,* 1964, 86 (8), 1642-1643. b) M. G. Davidson, M. A. Fox, T. G. Hibbert, J. A. K. Howard, A. Mackinnon, I. S. Neretin and K. Wade, Deboronation of *ortho*-carborane by an iminophosphorane: crystal structures of the novel carborane adduct *nido*-$C_2B_{10}H_{12}\cdots HNP(NMe_2)_3$ and the borenium salt $[(Me_2N)_3PNHBNP(NMe_2)_3]_2O^{2+}(C_2B_9H_{12}^-)^2$. *Chem. Comm.,* 1999, 1649-1650. c) M. A. Fox, W. R. Gill, P. L. Herbertson, J. A. H. MacBride, K. Wade and H. M. Colquhoun, Deboronation of C-substituted ortho- and meta-closo-carboranes using "wet" fluoride ion solutions, *Polyhedron*, 1996, 15, 565-571. d) M. A. Fox, J. A. H. MacBride and K. Wade, Fluoride-ion deboronation of p-fluorophenyl-ortho- and -meta-carboranes. NMR evidence for the new fluoroborate, HOBHF2-, *Polyhedron,* 1997, 16, 2499-2507. e) Y. Taoda, T. Sawabe, Y. Endo, K. Yamaguchi, S. Fujii and H. Kagechika, Identification of an intermediate in the deboronation of ortho-carborane: an adduct of ortho-carborane with two nucleophiles on one boron atom, *Chem. Comm*., 2008, 2049-2051. f) Y. Yoo, J. W. Hwang and Y. Do, Facile and mild deboronation of o-carboranes using cesium

fluoride, *Inorg. Chem*., 2001, 40, 568-570. g) L. I. Zakharki and V. N. Kalinin, Reaction of Amines with Barenes, *Tetrahedron Lett.,* 1965, 407-409. h) L. I. Zakharkin and V. S. Kirillova, Cleavage of Ortho-Carboranes to (3)-1,2-Dicarbaundecarborates by Amines, *Bull. Acad. Sci. USSR, Div. Chem. Sci.,* 1975, 24, 2484-2486. i) M. F. Hawthorne, D. C. Young, P. M. Garrett, D. A. Owen, S. G. Schwerin, F. N. Tebbe and P. A. Wegner, Preparation and Characterization of (3)-1,2- and (3)-1,7-Dicarbadodecahydroundecaborate(-1) Ions, *J. Am. Chem. Soc*., 1968, 90, 862-868.

[3] I. Bennour, A. Cioran, F. Teixidor and C. Viñas, 3,2,1 and stop! An innovative, straightforward and clean route for the flash synthesis of metallacarboranes, *Green Chem*., 2019, 21, 1925-1928.

[4] A. Zaulet, F. Teixidor, P. Bauduin, O. Diat, P. Hirva, A. Ofori and C. Viñas. Deciphering the role of the cation in anionic cobaltabisdicarbollide clusters, *J. Organomet. Chem*., 2018, 865, 214-225.

[5] T. Garcia-Mendiola, V. Bayon-Pizarro, A. Zaulet, I. Fuentes, F. Pariente, F. Teixidor, C. Viñas and E. Lorenzo, Metallacarboranes as tunable redox potential electrochemical indicators for screening of gene mutation, *Chem. Sci*., 2016, 7, 5786–5797.

[6] This article.

[7] I. Rojo, F. Teixidor, C. Viñas, R. Kivekäs and R. Sillanpää, Methylation and Demethylation in Cobaltabis(dicarbollide) Derivatives, *Organometallics*, 2003, 22, 4642-4646.

[8] L. Matel, F. Macásek, P. Rajec, S. Hermánek, J. Plesek. *Polyhedron* **1982**, *1*, 511-519.